Experimental and Computational Characterizations of Native Ligaments, Tendons, and Engineered 3-D Bone-Ligament-Bone Constructs in the Knee

by

Jinjin Ma

A dissertation submitted in partial fulfillment
Of the requirements for the degree of
Doctor of Philosophy
(Mechanical Engineering)
in The University of Michigan
2012

Doctoral Committee:

Professor Ellen M. Arruda, Co-Chair
Associate Professor Lisa M. Larkin, Co-Chair
Professor James A. Ashton-Miller
Associate Professor Scott Gregory McLean

Dedication

To my mom, dad, and my husband Yi

Acknowledgements

I would like to deeply thank my advisors Prof. Ellen M. Arruda and Prof. Lisa M. Larkin for their tremendous guidance, encouragement, support, and trust in me during the past five years. I am grateful to Ellen and Lisa for their knowledge and research skills. I am always encouraged and inspired by their passion towards research. I appreciate their brilliant ideas that they provided to me and their accessibility whenever I needed help and guidance. Especially I would like to thank Ellen for her willingness to have long discussions during our weekly or sometimes daily meetings. I would also like to thank Ellen for kindly supporting me to many conferences during the past five years. Through the conference opportunities, I have truly grown a lot professionally. Both Ellen and Lisa patiently guided me throughout the entire doctoral process, pushing me to achieve nothing but the best.

Next, I would like to thank Dr. Edward Wojtys for his guidance, encouragement, support, and kindness. I am very grateful to Dr. Wojtys for being extremely patient during the ACL surgery when I didn't know anything. I am also grateful for the time and energy he put on the ACL project. I appreciate all the beautiful histology work Prof. Tatiana Kostrominova provided for this project. I also appreciate the PCR work Prof. Deneen Wellik and her student Ilea Swinehart provided for this project. I would also like to thank my committee members, Prof. James Ashton-Miller and Prof. Scott Mclean for their suggestions and participations on my committee. I also appreciate Prof. Samantha Daly for her valuable advice on DIC Methods, and Prof. Krishna Garikipati for his valuable advice on finite element modeling. I would also like to thank Dr. Elizabeth Hildinger for her great support, encouragement, and kindness during my dissertation-writing period.

Next, I would like to thank my teammates, Mike Smietana and Hiroko Nakahama, who also have worked so hard on my projects. Thank you for always being there no matter how late the experiments went. Thank you for your flexibilities so that you were always available to help me whenever I needed help. I would not have accomplished the project without your help and support. I am also grateful to all STEL members and members in GGB 1025 and 3121, past and present, for your great support. I really enjoyed working with you guys. In particular, I am grateful to Sarah and Fatima for their guidance and great support during the initial stage of my projects. I would also like to thank Charlie, Kelly and Phil for their assistance.

Next, I would like to thank my friends in Ann Arbor, friends in graduate school and friends in Harvest Mission Community Church: Yipei, Astin, Aftin, Yu, Jess, Harish, Keqin, Siying, Rachel, Sarah, Shelly, Mirae, Kathleen, and many others. I appreciate so much for your love and support. I cherish our friendships so much and hope they shall always last.

Lastly, I would like to give my deepest appreciation to my parents and my husband Yi Liu. Without your trust, support, patience, and love, I could not overcome the hardships and difficulties I encountered during the past five years. I would like to thank my parents for constantly calling me to support and encourage me no matter how busy they are and where they are. I would like to thank Yi for cooking for months when I am busy. Thank you for your willingness to always work around my schedule. Thank you for always forgiving me when I lost control or my temper. Thank you for being such a perfect husband. To all of you, I dedicate this dissertation.

This work was financially supported by the Department of Mechanical Engineering, MICHR, Coulter Foundation, Rackham travel grant and Rackham graduate student research grant.

Table of Contents

List of Figures

Lists of Tables

CHAPTER 1

Introduction

1.1 Anterior cruciate ligament (ACL) and its tendon grafts

The anterior cruciate ligament (ACL) is one of four major ligaments that stabilize the knee. It has a complicated anatomic structure, inserting into the medial aspect of the lateral condyle of the femur and the anterior aspect of the tibial plateau [1-3]. Furthermore, the ACL is composed of multiple bundles of collagen fibers twisted together. It performs an important biomechanical function, restricting the anterior-tibial translation of the knee to within a normal range of motion [1-4].

Tears of the ACL are the most common knee injuries in sports according to recent statistics [7]. Knee injuries accounted for 400,000 physician office visits in the US in 2005 [5]. Worldwide, the proportion of knee injuries to young sports players that require surgery is estimated to be 17-61% [6], and in the US, knee injuries are now the leading cause of high school sports-related surgeries [7]. Without treatment to reconstruct the ACL, the patient will lose knee stability and experience abnormal knee kinematics. Over time, the patient may develop severe osteoarthritis (OA) that increases likelihood for total knee replacement [8-10]. Therefore an ACL reconstruction is needed to restore normal knee function. The current treatment is to use a tendon graft to replace the torn ACL. The rationale for this approach is that the microstructure of tendons is considered to be sufficiently similar to that of the ACL. ACL reconstruction surgeries, involving tendon autografts (i.e. tendon grafts obtained from patients' own tissue) or allografts (i.e. tendon grafts obtained from cadaver tissue), are performed in the

US at a rate of nearly 350,000 per year and acute care alone costs $6 billion annually [25]. Figure 1.1 demonstrates the ACL reconstruction procedure using a patellar tendon autograft [26]. In brief, the tendon graft is first procured from the patient (autograft) or a cadaver (allograft). Bone tunnels on the femur and tibia are drilled through the footprint of the ACL remnant. The tendon graft is then guided through the bone tunnels to replace the torn ACL. Fixation screws are used to secure the graft within the anatomic position in the knee with a small amount of tension.

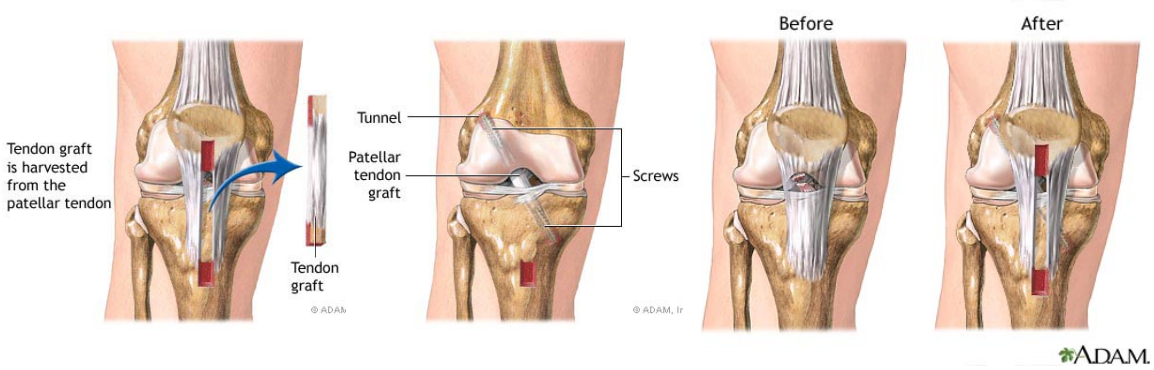

Figure 1.1 An ACL reconstruction procedure using patellar tendon autograft to replace the torn ACL.

Outcomes for ACL reconstruction using tendon grafts are limited by graft availability, risk of rejection, and increased donor site morbidity. In addition, the region of the graft within the bone tunnel does not fully integrate with native tissue and the grafts are poor biomechanical matches for the ACL [7, 8, 11]. Graft failure rates are 25% for the youngest, most active patients [12]. Moreover, acute ACL injuries are increasingly becoming more prevalent in children as young as 12 years old, which means they have a high likelihood of developing OA before age 20 and living with the debilitating effects of this condition for the rest of their lives. Clearly there exists a need for an engineered ligament that will develop biochemically relevant and biomechanically compatible interfaces with native tissue and restore the proper biomechanics to the knee.

In recent decades, researchers have been investigating tissue engineering strategies that will lead to better ACL surgical outcomes. Current tissue engineering methodologies utilize various biocompatible scaffolds,

fibroblasts or mesenchymal stem cells, and growth factors that promote cell proliferation and differentiation to engineer grafts *in vitro* [13-15]. While these tissue engineered scaffolds have many advantages, limitations such as undesirable degradation rates of the scaffolds, immediate cell death after implantation, and mis-matched biomechanical properties hinder their ability to develop into a mature tissue that can replace the native ACL [16]. Therefore, there is a need to improve the current tissue engineering strategies so that the engineered graft can be biocompatible, is capable of fully integrating to native bone, rapidly remodels *in vivo,* and ultimately matches native biomechanical properties.

1.2 Characterization of ligaments and tendons

In order to understand and evaluate the efficacy of tissue engineered grafts, we need to provide means to characterize the mechanical responses of native and engineered ligaments and tendons experimentally, to establish constitutive models that describe accurate mechanical responses of these tissues, and to construct a finite element model that is integrated with accurate geometry and constitutive relationships provided by the previous steps.

1.2.1 Experimental characterization

A variety of mechanical experiments is carried out with the aim of understanding and evaluating the functions and biomechanical properties of the ACL, tendon grafts, and tissue engineered grafts. Extensive human cadaver studies and animal studies have been conducted to elucidate their biomechanics [17-21]. Several types of experiments, including laxity tests, in situ force tests, uniaxial tension tests, and viscoelastic tests, have been conducted to study the tissues' functional properties and nonlinear viscoelastic mechanical behaviors. Although these tests are standard, because of the intrinsic properties of these tissues such as anisotropy, inhomogeneity, and multi-directional fiber orientation, experiments that take these limitations into consideration are needed to elucidate the biomechanical properties of the soft tissues.

1.2.2 Constitutive models

Once measurements are obtained from experiments, the information can then be used to establish constitutive relationships for native and engineered tissues in order to (1) evaluate whether current tendon grafts or tissue engineered grafts have optimal mechanical function for implantation and utility for regenerative medicine and (2) establish stress-strain relationships to prescribe accurate tissue response in finite element studies. The quasi-linear viscoelastic (QLV) formulation by Fung 1972 and a modified constitutive model based on the QLV theory have been used extensively to quantify the nonlinear viscoelastic properties of the tissue [22]. However, recent studies have demonstrated that these QLV based models do not fully describe the viscoelastic behaviors of ligaments and tendons at lower strain or stress ranges. Other models have been proposed to capture the viscoelastic responses of ligaments and tendons, such as the modified superposition theory by Provenzano et al., 2002 and Oza et al., 2003 [23, 24]. While these curve-fitting models capture the ligament and tendon responses, it is important to realize that the mechanical responses of these tissues are modulated by the content and morphology of structural proteins such as type I collagen and elastin, other molecules such as glycosaminoglycans, and fluid. Therefore, microstructural constitutive models ultimately can provide a better relationship between the mechanical response and the microstructure of the tissue using physically relevant parameters.

1.2.3 Finite element models

Constitutive information can then be fed into a finite element model to study the mechanical responses of the tissues in 3D physiological settings. Eventually, the finite element model can be a useful tool to provide much insight into the function and failure mechanisms of native and engineered ligaments and tendons.

1.3 Aim and outline of this thesis

For my dissertation, I have pursued a paradigm for ACL reconstruction

pioneered in our laboratory that involves *in vitro* tissue engineering of a scaffold-free multi-phasic construct from bone marrow stromal cells (BMSC). The innovative aspects of this approach include the scaffold-free technology itself, the development of a patient-specific, off-the-shelf technology for complete ACL recovery, an engineered interface between the intra-articular region and the bone *in vitro*, engineered bone ends for placement into the bone tunnel regions that fully integrate with the native tissue,and a redesign of the mechanical properties needed at the time of implantation for the intra-articular region to reduce or eliminate the body's initial degradation of the reconstructed tissue, and to quickly and completely restore the original biomechanics to the knee joint.

The aim of this work is to understand and describe the biomechanics of native and engineered ligaments and tendons both experimentally and constitutively, and to examine the biomechanical responses of the native ACL, tissue engineered ACL, and tendon grafts in a 3D physiological setting in the knee joint. To achieve this aim, we designed and fabricated tissue engineered bone-ligament-bone constructs. The efficacy of their ability to replace native tissue was demonstrated as a native tissue replacement in rat and sheep models. We then designed and conducted experiments that characterize the nonlinear viscoelastic mechanical properties of native and engineered ligaments and tendons taking the inhomogeneous geometry of the native tissue into consideration. Furthermore, we established a physiologically relevant constitutive model to analytically describe the nonlinear viscoelastic properties of native and engineered ligaments and tendons. Finally, we have implemented the microstructural-based constitutive model into a 3D finite element setting to understand the biomechanical response of these tissues in a complicated physiological loading condition.

In this thesis, **Chapter 2** presents a review of the current understanding of the anatomy of the native ACL, the ACL tear mechanism, and current ACL reconstruction approaches. The subsequent chapters of this thesis present the

four main building blocks of this work. In **Chapter 3**, we report on our scaffold-less tissue engineered 3D bone-ligament-bone constructs fabricated to replace the native MCL in rat model and native ACL in sheep model. **Chapter 4** details experiments we designed to accurately characterize the material properties of native and engineered ligaments and tendons. The experimental results provided by these experiments were then used to establish a microstructural-based constitutive model, presented in **Chapter 5**, that describes the mechanical responses of soft tissue from a physiological point of view. In **Chapter 6**, the constitutive model was further developed and implemented into a finite element model with improved ACL geometry in the knee. This model was applied to reveal the biomechanical response of the native and engineered ligaments and tendons in complicated physiological loading conditions. The last part of this thesis, Chapter 7, provides a summary of the thesis along with limitations and suggestions for future studies that will strengthen the findings.

1.4 References

1. Girgis, F.G., J.L. Marshall, and A. Monajem, *The cruciate ligaments of the knee joint. Anatomical, functional and experimental analysis.* Clinical orthopaedics and related research, 1975(106): p. 216-231.

2. Arnoczky, S.P., *Anatomy of the anterior cruciate ligament.* Clinical orthopaedics and related research, 1983(172): p. 19-25.

3. Amis, A.A. and G.P. Dawkins, *Functional anatomy of the anterior cruciate ligament. Fibre bundle actions related to ligament replacements and injuries.* The Journal of Bone and Joint Surgery, 1991. **73**(2): p. 260-267.

4. Butler, D.L., M.D. Kay, and D.C. Stouffer, *Comparison of Material Properties in Fascicle-Bone Units From Human Patellar Tendon and Knee Ligaments.* Journal of Biomechanics, 1986. **19**(6): p. 425-432.

5. Annual Meeting of American Orthopaedic Society of Sports Medicine, *Sports Medicine. Keystone (CO), July 14–17.* 2005.

6. Louw, Q.A., J. Manilall, and K.A. Grimmer, *Epidemiology of knee injuries among adolescents: a systematic review.* British Journal of Sports Medicine, 2008. **42**(1): p. 2-10.

7. Ingram, J.G., et al., *Epidemiology of knee injuries among boys and girls in US high school athletics.* The American Journal of Sports Medicine, 2008. **36**(6): p. 1116-22.

8. Roos, E.M., *Joint injury causes knee osteoarthritis in young adults.* Current opinion in rheumatology, 2005. **17**(2): p. 195-200.

9. Selmi, T.A.S., D. Fithian, and P. Neyret, *The evolution of osteoarthritis in 103 patients with ACL reconstruction at 17 years follow-up.* Knee, 2006. **13**(5): p. 353-358.

10. Kessler, M.A., et al., *Function, osteoarthritis and activity after ACL-rupture: 11 years follow-up results of conservative versus reconstructive treatment.* Knee surgery, sports traumatology, arthroscopy : official journal of the ESSKA, 2008. **16**(5): p. 442-8.

11. Scheffler, S.U., F.N. Unterhauser, and A. Weiler, *Graft remodeling and ligamentization after cruciate ligament reconstruction.* Knee Surgery, Sports Traumatology, Arthroscopy, 2008. **16**(9): p. 834-842.

12. Kaeding, C.C., D. Flanigan, and C. Donaldson, *Surgical Techniques and Outcomes After Anterior Cruciate Ligament Reconstruction in Preadolescent Patients.* Arthroscopy : The Journal of Arthroscopic & Related Surgery : Official Publication of the Arthroscopy Association of North America and the International Arthroscopy Association, 2010. **26**(11): p. 1530-1538.

13. Ge, Z., et al., *Biomaterials and scaffolds for ligament tissue engineering.* Journal of biomedical materials research.Part A, 2006. **77**(3): p. 639-652.

14. Laurencin, C.T. and J.W. Freeman, *Ligament tissue engineering: an evolutionary materials science approach.* Biomaterials, 2005. **26**(36): p. 7530-7536.

15. Cooper, J.A., Jr., et al., *Biomimetic tissue-engineered anterior cruciate ligament replacement.* Proceedings of the National Academy of Sciences of the United States of America, 2007. **104**(9): p. 3049-54.

16. Mascarenhas, R., *Anterior cruciate ligament reconstruction: a look at prosthetics-past, present and possible future.* McGill Journal of Medicine, 2008. **11**(1): p. 29-37

17. Noyes, F.R. and E.S. Grood, *Strength of Anterior Cruciate Ligament in Humans and Rhesus-Monkeys.* Journal of Bone and Joint Surgery-American Volume, 1976. **58**(8): p. 1074-1082.

18. Woo, S.L., et al., *Tensile properties of the human femur-anterior cruciate ligament-tibia complex. The effects of specimen age and orientation.* The American Journal of Sports Medicine, 1991. **19**(3): p. 217-25.

19. Danto, M.I. and S.L. Woo, *The mechanical properties of skeletally mature rabbit anterior cruciate ligament and patellar tendon over a range of strain rates.* Journal of orthopaedic research : official publication of the Orthopaedic Research Society, 1993. **11**(1): p. 58-67.

20. Chandrashekar, N., et al., *Sex-based differences in the tensile properties of the human anterior cruciate ligament.* Journal of Biomechanics, 2006. **39**(16): p. 2943-50.

21. Butler, D.L., *Anterior cruciate ligament: Its normal response and replacement.* Journal of Orthopaedic Research, 1989(7): p. 910-921.

22. Y.C., F., *Stress-Strain-History Relations of Soft Tissues in Simple Elongation*. Biomechanics: Its Foundation and Objectives, 1972, Englewood Cliffs, NJ: Prentice-Hall.

23. Oza, A.L., R. Vanderby, and R.S. Lakes, *Creep and relaxation in ligament: Theory, methods and experiment*, ed. G.A. Holzapfel and R.W. Ogden, 2006. 397.

24. Provenzano, P.P., et al., *Application of nonlinear viscoelastic models to describe ligament behavior.* Biomechanics and modeling in mechanobiology, 2002. **1**(1): p. 45-57.

25. National Center for Health Statistics, National Ambulatory Medical Care Survey, 2004. Available on the American Association of Orthopaedic Surgeons web page at aaos.org.

26. http://www.wakehealth.edu/Health-Encyclopedia/Presentations/Anterior-Cruciate-Ligament-Repair---Series.htm

CHAPTER 2

Background and Motivation

The anterior cruciate ligament (ACL) is a major knee ligament that stabilizes the knee by connecting the femur and the tibia in the knee joint. The main function of the ACL is to maintain the normal range of motion during knee anterior-tibial translation. The ACL has a complicated anatomic structure. It is composed of multiple collagen bundles twisted together. Limited amount of vascularization and innervation are found in the ACL. Because of its intrinsic anatomic structure, the self-healing ability of the ACL is poor. The ACL is commonly injured in high impact sports during acceleration or deceleration with or without a direction change. Because of its poor self-healing ability, a surgical procedure to reconstruct the ACL is required to replace the torn ACL in order for patients to recover and regain normal physical activity. Without surgery, patients lose knee stability and experience abnormal knee kinematics. Over time, patients may develop severe osteoarthritis and face the possibility of needing a total knee replacement. Therefore, to reduce or eliminate these limitations, investigators are motivated to seek other solutions and strategies to reconstruct the torn ACL. Understanding the ACL anatomical structure, its function, and the interrelation between the structure and the function thus become critical for further investigation.

2.1 ACL Anatomy and Function

Ligaments and tendons are connective tissues that consist of cells and the extracellular matrix secreted by these cells. The major component of the extracellular matrix is collagen. Ligaments and tendons connect bone to bone (ligaments) or connect muscle to bone (tendons) and transmit forces and

maintain normal range of joint motion. The anterior cruciate ligament (ACL) is one of four major knee ligaments and it resides in the intra-articular region of the joint (Figure 2.1). In addition to its complicated bone-ligament interfaces, the ligament portion of the ACL has a complex, inhomogeneous geometry. This complex structure leads to its nonlinear, anisotropic, and viscoelastic biomechanical properties.

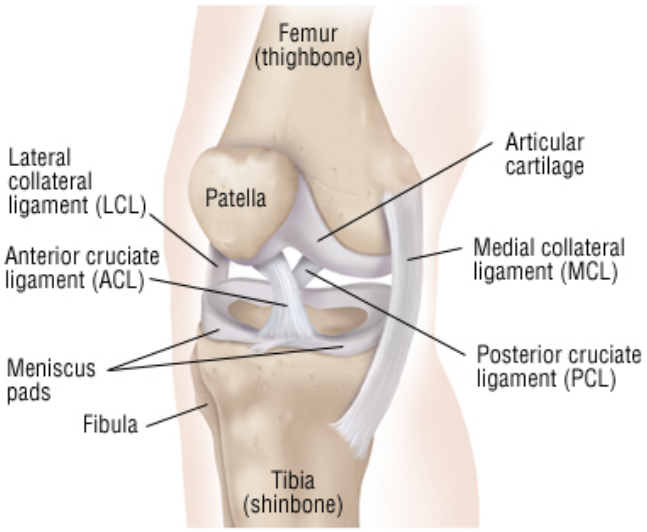

Figure 2.1 Anatomical structure of a human knee [92].

2.1.1 Macroscopic anatomy of the ACL

The ACL originates from the posterior aspect of the lateral femoral condyle and inserts into the lateral aspect of the tibia plateau. Furthermore, the ACL twists on itself in a slight lateral spiral [1, 2]. The ACL attaches to the femur and tibia as a collection of individual fascicles that fan out over a broad flattened area. These fascicles are oriented in different directions. Some fascicles are orientated in a spiral pattern along the long axis of the ACL; others are directly connected from femoral to tibial attachment [1]. Hara et al., 2009 traced these fascicular structures and they demonstrated that these fascicles twist around each other when the knee flexes [3]. Specifically, the ACL is attached to the posterior aspect of the medial surface of the lateral femoral condyle with a semi-elliptical footprint shape (Figure 2.2 **A**) [4]. The ACL fans out as it approaches the tibia. It then attaches to the depressed area of the anterior and lateral aspect of

the tibia with an irregular footprint (Figure 2.2 **B**) [4]. The depressed area is approximately 11 mm wide and 17 mm antero-posteriorly [2, 4, 5]. The shape and area of the cross section of the ACL changes along the long axis of the ACL [2]. The cross sectional area of the ACL is the smallest near the femoral insertion site and the largest near the tibial insertion site [2]. This suggests that the tibial attachment of the ACL would be stronger than the femoral attachment if the material properties were uniform along the length of the ACL [6]. When the knee is in the extended position, the ACL is flat. When the knee is flexed, the ACL begins to wind and bundles become twisted around one another (Figure 2.3). The average length and width of the ACL reported from the literature are 32 mm and 11 mm, respectively [5].

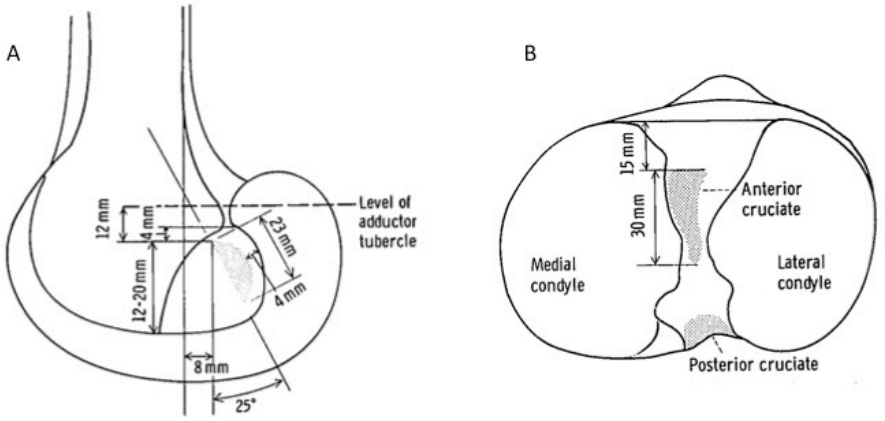

Figure 2.2 ACL insertions and bone attachment on femur (A) and on tibia (B) [4].

Because of the complicated bone attachments of the ACL, not all of its fascicles present the same tightness or looseness at the same knee flexion angle [4], suggesting these fascicles may be divided into functional groups for better ACL functional and biomechanical response. Chhabra et al., 2006 demonstrated that the fetal human ACL has separate fiber bundles during embryogenesis [7]. This separation is found consistently in old age [8, 9]. Therefore, investigators have treated the structure of the ACL as separate fascicle bundles. While Norwood and Cross 1979, Rosenburg and Rasmussen 1984, and Amis et al., 1991 have treated the ACL as three functional bundles, - anteromedial, intermediate, and posterolateral [5, 8, 10], Girgis 1975 and Arnoczky 1983 have

divided the ACL into two bundles - the anteromedial bundle (AMB) and the posterolateral bundle (PLB) [4, 6]. The AMB originates at the most anterior and proximal aspect of the femur and inserts at the anteromedial aspect of the tibia, while the PLB originates at the postero-distal aspect of the femor and inserts at the posterolateral aspect of the tibial attachment [4]. The PLB contains more collagen fibers than that of the AMB [5]. The less common three-bundle treatment first also divides the ACL into anterior and posterior bundles. The anterior bundle is then subdivided into medial and lateral halves [11, 12].

While both characterizations are applied to the ACL, the two bundle separation is found to be more widely accepted and used to characterize the ACL, and is supported by recent arthroscopic analysis performed by Steckel 2009 [13] and the well-defined two-bundle structure found in fetal ACLs [14].

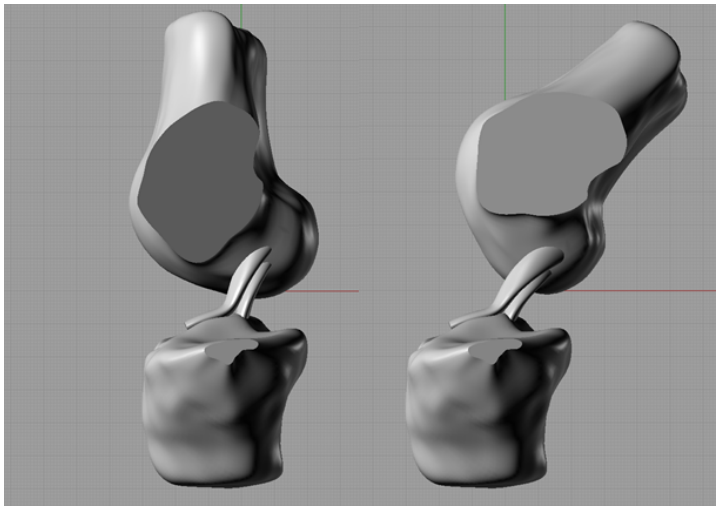

Figure 2.3 Schematic drawing represents changes in the shape and the tension of the ACL in extension and flexion due to the femur attachment.

During knee extension, the two bundles run relatively parallel to one another. During knee flexion, the AMB spirals around the PLB [2]. This is due to the femoral attachment of the ACL and the significant length differences in the two bundles, which leads to complex, non-uniform strain patterns on the ACL bundles in various knee positions [15]. As the knee is extended the PLB is strained, while the AMB is lax. As the knee is flexed, the femoral and tibial

attachments of the PLB move closer to each other, resulting in a PLB that is unloaded and lax. On the contrary, the attachments of the AMB move away from each other during flexion, causing the AMB to become taut and strained [4, 6]. Arnoczky 1983 also noted that the afroementioned description oversimplifies the orientation of the ACL. The ACL is a continuum of fascicles and in any position of knee flexion-extension, there is always a portion of the ACL that remains under tension and provides knee stability [6].The fascicles from the convex border form the medial side of the ligament and are attached to the anterior tibial spine. They stand out as a thin single band. This band is tense in flexion [4].

2.1.2 Micro anatomy of the ACL

Like other dense connective tissue, the ACL consists of cells and an extracellular matrix secreted and maintained by these cells. The major cell type in the ACL is spindle-like fibroblasts. The round or ovoid shaped cells that resemble chondrocytes (commonly present in fibrocartilage) are also found in the ACL [16]. Myofibroblasts-like cells (commonly present in muscle) that contain alpha-smooth muscle actin are also found in the midsubstance of the intact human ACL [17]. The extracellular matrix of the ACL is composed of four different constituents, namely collagen (Type I collagen dominates with limited amounts of type II, III, IV and VI collagen), glycosaminoglycans (GAGs), glyco-conjugates (laminin, entactin, tenascin, and fibronectin), and elastin [2].

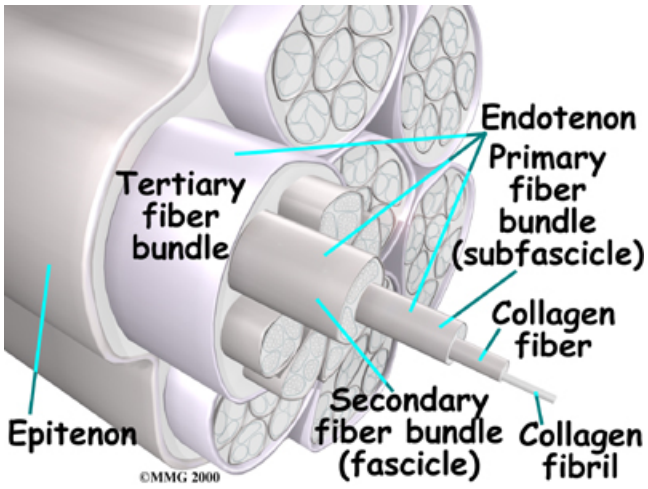

Figure 2.4 Collagen fascicle structure in tendons and ligaments [95]

The major component in the extracellular matrix of the ACL is collagen. The structure of collagen can be described hierarchically [1]. As shown in Figure 2.4, the ACL is made up of multiple fascicles that can be grouped into bundles (AMB and PLB) as described previously. The substructures within these fascicles are collagen fibrils that have a large range of diameters. The smallest diameter reported is 25 nm [18], and the largest 250 nm [1, 2, 16]. These collagen fibrils form nonparallel, interlacing networks, and the fibrils are grouped into fibers that have 1-20 μm diameters. The fibers form subfascicles with a 100-250 μm diameters, each surrounded by a loose band of connective tissue known as the endotenon. Three to twenty subfascicles bound together to form a fascicle, which may range from 250 μm to several mm in diameter and is surrounded by an epitenon. The entire continuum of fascicles is grouped into two major bundles to form the ACL. Another connective tissue layer, the paratenon, surrounds the entire ACL [1, 6].

Strocchi et al., 1992 have characterized two types of fibrils in the ACL. The first type of fibril is secreted by fibroblasts, has a diameter ranging from 25 to 85 nm, and an irregular cross section profile. This type of fibril accounts for 50.3% of the entire ACL and is specialized to resist high tensile stresses. The second type of fibril is secreted by fibro-chondroblasts. It has a uniform diameter (45 nm) and a smooth cross section profile. This type of fibril is believed to maintain the three-dimensional organization of the ligament [18]. Elastin is found abundantly in both transverse and longitudinal sections of the ACL.

The cross-section of the ACL reveals collagen fascicles and connective sheaths. The ratio between the areas occupied by these two structures varies along the length of the ACL [1], suggesting the micro anatomy of the ACL may vary along the length of the ACL. Transmission electron microscopy images have revealed that the collagen fibrils located in different regions of the ACL possess different diameters as shown in Baek et al., 1998 [19]. In their study, collagen fibril diameters in the ACL from young human specimens (17-22 years) were found to be largest in the distal region (78.2 ± 29.7 nm) but decreases proximally

(middle: 74.8 ± 27.6nm; proximal: 66.1 ± 26.4nm) [19]. Duthon et al., 2005 have established a detailed study to characterize the microstructure of the ACL regionally [2]. Specifically, this study analyzes the microanatomy of the ACL by distinguishing the ACL into proximal, middle, and distal zones, to identify the extracellular components in each zone. Their key results are as follows:

1. *The proximal zone* is highly cellular with round and ovoid cells. This zone is composed of fusiform fibroblasts, collagen type II and glycoproteins such as fibronectin and laminin [2].

2. *The middle zone* contains fusiform and spindle-shaped fibroblasts, elastic and ocytalan fibers along with a high density of collagen fibers. This zone also contains cartilage and fibrocartilage. The fusiform and spindle-shaped fibroblasts are dominant. The densest zone of fibroblasts is located in the middle and proximal one-quarter of the ACL, with cells and blood vessels longitudinally oriented and high crimp length [2].

3. *The distal zone* of the ACL is rich in chondroblasts and ovoid fibroblasts. The collagen bundle density is relatively low in this zone [2]. Petersen et al., 1999, demonstrated that this fibrocartilaginous zone is located 5-10 mm proximal of the tibial ligament insertion on the anterior portion of the ACL [16]. The cells in this area are chondrocyte-like. The collagen fascicles in this region cross each other at sharp angles [16]. The diameters of these fibrils are between 130 to 250 nm, larger than elsewhere in the ACL [2][16]. In a knee extension position, the intercondylar fossa of the femur may cause a compressive strain on the anterior part of the ACL. Therefore, the fibrocartilage region in the ACL may be formed to withstand the compression generated [16, 20].

The insertion site of the ligament to bone is called the *enthesis*. It has a unique microstructure to mitigate the stress concentration as the soft ligament tissue transitions to hard bone. The ligament transitions to bone via a transitional zone of fibrocartilage and mineralized fibrocartilage [6]. The gradual structural alteration in the transitional zone allows for a gradual change in stiffness and prevents stress concentration at the attachment site [6]. Benjamin et al., 2006

classified the entheses into *fibrous* and *fibrocartilaginous entheses* according to the type of tissue present at the insertion sites [21]. At *fibrous entheses*, the tendon or ligament attaches either directly to the bone or indirectly to it via a structure called *Sharpey's fibers* (a term used to designate collagen bundles from tendon/ligament microstructures penetrating to bone structure) [21, 22]. This type of enthesis usually connects tendon/ligament to a membranous bone. Whereas at *fibrocartilaginous entheses*, chondrogenesis occurs and four zones of tissue can be detected, namely pure dense fibrous connective tissue, uncalcified fibrocartilage, calcified fibrocartilage, and bone. This type of enthesis usually connects tendon/ligament to an endochondral bone [21, 22]. Though it is difficult to precisely define the beginning or the end of the entheses, a tidemark, the basophilic line separating the uncalcified zone and calcified fibrocartilage zones, can be identified [21]. Calcified fibrocartilage is typically less cellular than the uncalcified portions of the rest of enthesis. It is believed the fibrocartilage is differentiated from tendon/ligament cells at the enthesis by changing cell shape and cell-cell interactions [20, 23]. This tissue expresses cartilage markers such as type II collagen and aggrecan [21, 24]. All fibrocartilage associated with normal entheses is believed to be avascular which leads to the poor self healing response of the ACL at and near the attachment sites [21].

The entheses of the ACL is 100 um to 1 mm in length on average depending on species and age [16, 25, 26]. Few studies have shown the detailed microstructure of the ACL enthesis. Petersen et al., 1999 detected mineralized fibrocartilage in both femoral and tibial entheses [16]. Scranton et al., 1998 detected Sharpey's fibers at the ACL graft (quadruple-hamstring) insertions in both sheep and human specimens as early as 6 weeks [94]. These studies indicate that both fibrocartilage and Sharpey's fibers can be used to detect the biological anchoring formation of the ACL graft to the host bone.

2.1.3 Vascularization and innervation

2.1.3.1 Vascularization

Arnoczky 1983 summarized that the blood vessels in the ACL are likely from the periligamentous vessels formed by the synovial fold that covers the ACL [6]. These periligamentous vessels form smaller connecting branches and penetrate the ligament transversely with a network of endoligamentous vessels. The vessels, along with their supporting connective tissues, are oriented in a longitudinal direction and lie parallel to the collagen bundles within the ligament [6].

The ACL vascular supply is not sparse even within the deepest layer of the ligament and it is suggested it is adequate for healing of the ligament [6, 27]. However, the blood distribution within the ACL is not homogenous, with better vasculature supply in the proximal part of the ACL than the distal part of the ACL. The fibrocartilagious part of the ACL is avascular [16]. This is believed to play a role in the poor healing potential of the ACL [2].

2.1.3.2 Innervation

The ACL receives nerve fibers from branches of the tibial nerve. These fibers penetrate the joint capsule posteriorly and move along with the synovial and periligamentous vessels surrounding the ligament. Smaller nerve fibers have also been observed throughout the substance of the ACL. In addition, some singular nerve fibers without tibial origins have been found among the fascicles of the ligament and it is possible that these fibers contribute to sensory function by functioning as receptors [6, 27, 28]. Recent data also suggest these sensory receptors in the ACL may play an important role in the arthrokinetic reflex that contributes to overall neuromuscular control of the knee joint [29]. It is believed that the ACL reflex is essential in normal knee function [30, 31]. This feedback is lost in patients with a ruptured ACL, which leads to femoral weakness in the quadriceps [31].

2.1.4 ACL function

The anatomy and spatial orientation of the ACL within the joint can be directly related to its function as a constraint to joint motion. For detailed anatomical structure of the ACL, please refer to section 2.1.1. Briefly, the femoral and tibial attachments of the ligament, as well as the multifascicular nature of its structure, allow different portions of the ligament to be taut, and therefore functional, throughout the range of motion [6]. Studies have been performed in the past few decades with the goal of elucidating the complicated function of the ACL [4-6, 15, 32]. Early studies examined the role of the ACL by performing an anterior tibial displacement or drawer test on the cadaver knee before and after the ACL was cut [4, 32]. When all elements in the knee are intact, detection of the sliding movement of the anterior femur along the tibia is limited. However, when the ACL is cut and all other elements in the knee capsule were kept intact, the knee could easily be hyperextended. Both internal and external rotations of the tibia are also increased with in the absence of an intact ACL [4]. The ACL is a primary restraint to knee anterior tibial displacement [32 and references within]. The ACL is taut when the knee is in full extension and at 5 and 20 degrees of flexion. It becomes more relaxed between 40 and 50 degrees of flexion, and then becomes increasingly taut as flexion is increased from 70 to 90 degrees [6].

It is suggested that the AMB of the ACL is responsible for the increase in antero-posterior drawer with flexion [4]. Butler, 1989 concluded that the anterior bundle provides all of the anterior restraining action at a 30 degree flexion angle [33]. Amis et al., 1991 demonstrated that the PLB contributed the most (47%) to force resistance measured at a 20 degree knee flexion angle. They reported that the posterior bundle slackens in flexion, leaving the anteromedial bundle to resist anterior tibial translation in the knee at 90 degree flexion [5]. Hefzy et al., 1987 have showed that the ligament insertion portions change very little in strain during knee flexion-extension [34]. However, Bulter 1989 showed that if tested in a uniaxial tension setup, the ligament insertion site experiences more strain whereas in the middle there is little strain, indicating the middle portion of the

ACL is stiffer than that of the insertions [32]. Hollis et al., 1991 designed a kinematic linkage device, a 6-degree of freedom robotic system, to measure knee joint motion. As stated in their study, when measuring the length of each ACL sub-bundle, the bundles are often assumed to be a straight line connecting the femur and tibia. This assumption leads to an underestimation of the true ACL length change since the fibers are usually twisted resulting in longer contour lengths [15]. Hollis et al., 1991 divided the ACL into three bundles and found that through the 0-90 degree knee flexion span, the antero-medial (AM) bundle gradually lengthened while the postero-lateral (PL) bundle gradually shortened and the intermediate (IM) bundle did not change in length. At zero external load condition (30 degree knee flexion), the AM bundle was lengthened while the PL portion is shortened and the IM portion did not significantly change in length. With an anterior load, the AM portion lengthened slightly less than the PL portion [15]. Finally, in a recent review, Amis 2012 concluded that the AM bundle contributes the most to resisting tibial anterior translation, which is the primary function of the ACL. When the knee is at extension, the PL bundle of the ACL tightens so that the ACL also has a role in controlling tibial rotational laxity [35].

Bach et al., 1997 implanted strain gauges in the AM and PL bundles to measure the changing strain during knee flexion motion [51]. They found that the AM bundle has very little change (<1%) from 10 to 90 degrees knee flexion while the PL bundle was relaxed from 40 degrees onward. At 8 degrees hyperextension, the AM bundle was stretched 4% beyond its initial length while the PL bundle elongated by 10% of its initial length [51]. The data were confirmed by the recent studies using 3D imaging methods *in vivo*. Zantop et al., 2005 reported that after the PL bundle is dissected, anterior tibial transition became larger than that of an intact knee at 30 degree knee flexion after an anterior tibial load, but no difference was found at 60 and 90 degree knee flexions. Whereas after the AM bundle is dissected, the anterior tibial transition was larger than that of both an intact knee and the PL bundle dissected knee at 60 and 90 degree, but no differences were found between 0 to 30 degree knee flexion [36].

2.1.5 The biomechanical properties of the ACL

Many biomechanical studies have been performed to characterize the structural and material properties of the ACL. Several measurements are used to characterize the ACL, including geometric stiffness, tangent modulus, failure strength, strain to failure, and failure mode [37-42]. A typical dense connective tissue demonstrates a nonlinear viscoelastic stress vs. strain relationship. Traditionally, the mechanical properties of the ACL are characterized from a load to failure curve (Figure 2.5), in which load and displacement are direct measurements from instruments. From the load vs. displacement curve, one can measure the geometric stiffness - a property that is dependent on the size of samples tested - to ultimate load (load to failure), and ultimate displacement (displacement at the ultimate load). The load and displacement are then converted to nominal strain and nominal stress to characterize material properties such as tangent modulus, ultimate stress (stress to failure) and ultimate strain (strain at ultimate stress).

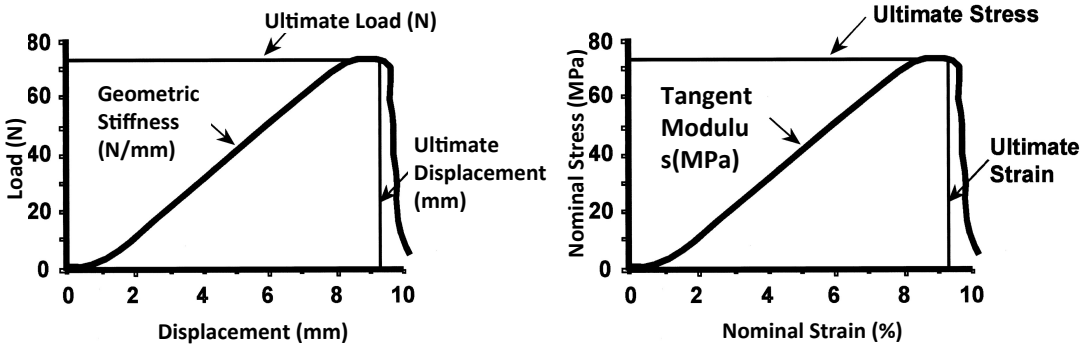

Figure 2.5 A representative load vs. displacement curve (left) and the nominal stress vs. strain curve (right) of a typical dense connective tissue (tendon or ligament). Figures adapted from Woo et al., 1999 [43].

The biomechanical properties of the human ACL have been extensively studied and study results are summarized in **Chapter 4** Table 4.1 and Table 4.1. A detailed description of the two tables and a thorough discussion characterizing the biomechanical properties of tendons and ligaments including ACL can be

found **in Chapter 4.** The average geometric stiffness of the human ACL is 178 N/mm and the average tangent modulus is 106 MPa; load to failure is 1061 N and the corresponding strain to failure of the human ACL is 20%. The structural characteristics of the ACL support its function as sustaining multi-axial stress. Butler et al., 1992 divided the ACL using a three-bundle model and measured the tangent moduli of all three subunits. They found that while the strain at failure is quite similar (15% to 18%), the two anterior bundles failed at higher tangent moduli with higher maximum stresses than those of the posterior bundle [11]. The authors hypothesized the mechanism causing different tangent moduli in bundles might be the frequency of loading. *In vivo*, anterior bundles are more frequently loaded than posterior bundles, which may lead to the development of the higher modulus. As discussed earlier, the microscopic anatomy of the ACL shows that fibrocartilage zones are found at the anterior portion of the ACL, which may also cause the anterior bundles to experience higher stresses. The fact that all bundles failed at a similar strain level suggests the ACL fails by a strain-dependent mechanism [11].

The biomechanical properties of the ACL/bone entheses have also been examined recently. Four zones in the ACL entheses previously described (section 2.1.2) have region-dependent mechanical properties that correlate to their mineral contents [26]. The study also reported that the mechanical properties of the ACL femoral and tibial entheses are significantly different, even though both entheses have similar histological properties and extracellular component contents. It is suggested that the difference in collagen fiber organization in the two entheses may contribute to the insertion site-dependent mechanical properties [26].

2.2 ACL Injuries

Knee injuries accounted for 400,000 physician office visits in the US in 2005 [44]. Worldwide, the proportion of knee injuries to young sports players that require surgery is estimated to be 17-61% [45], and in the US, knee injuries are

now the leading cause of high school sports-related surgeries [46]. Among all knee injuries, anterior cruciate ligament (ACL) injury is the most common. The incidence of ACL injury has been estimated at one in 3000 Americans [47]. These numbers are up 3-4 fold from estimates from about a decade ago and are increasing rapidly in pre-teens and teenagers [70].

2.2.1 Diagnosis and ACL tear patterns

Physical examination such as the anterior drawer test and the Lachman pivot shift test, devices designed to quantify anterior tibial translation (TK series arthrometer), advanced imaging (CT and MRI), and direct arthroscopic examination are used to assess the ACL tear [48].

Even though large stress concentrations at the entheses could make the ACL vulnerable to acute or overuse in sports [21], ACL tears with bone avulsion are very uncommon [27]. The mid-portion of the ligament and the proximal end of the ligament near the femur were demonstrated to be the most common sites of ACL tears [27]. The tear site makes the reattachment of the ligament to its femoral origin difficult. Various types of ACL tear patterns have been documented including complete ruptures, and partial tears with sub-division of AM and PL tears. A recent study arthroscopically identified that 21.2% of ACL tears are partial tears. Within this subgroup, 8.6% were PL bundle tears while the remaining 12.6% were AM bundle tears. This study utilized 174 patients who underwent ACL reconstruction [49]. Another study of 169 patients recorded the majority had complete ACL ruptures, 13 cases had an AM bundle rupture and 4 cases had a PL bundle rupture [50]. In a recent study, Zantop et al., 2007 reported that among 121 patients undergoing ACL reconstructions, 25% were partial tears whereas the rest were complete ACL ruptures. In 44% of all patients, AM and PL bundles did not rupture at the same location, while 56% of the patients did experience AM and PL rupture at the same location, a proximal tear. No sign of PL rupture was observed in 12% of the patients, however, no patients had an intact AM bundle [65].

2.2.2 ACL tear mechanisms

When the strain or stress developed along the ACL fascicles is beyond their limit, partial groups or the entire continuum of fascicles tear. ACL functions within a small range of tensile strains and typically ruptures at 20% strain [35].

Approximately 70% of ACL injuries are caused from noncontact injuries [52]. The cause of the ACL tear has been characterized as a combination of external-rotation and abduction forces, or a hyperextension, or by an anteriorly directed force applied to the posterior aspect of the tibia. It has recently been suggested that ACL injury is possible via a purely sagittal plane loading mechanism [53]. Terauchi et al., 2011 claimed that the majority of athletes indicate a close to full extension knee position at the time of injury [54]. Many researchers speculate that a more complex three-dimensional scenario leads to the ACL tear [55]. Impact-induced tibiofemoral accelerations during a landing may cause ACL elongation to rupture [56]. Kennedy et al., 1974 suggested that one mechanism that causes an isolated ACL tear is an internal rotation of the tibia on the femur, however, this proposed mechanism cannot be reproduced in the laboratory using cadaver knees [27]. The orientations of ACL attachments are dependent on whether their point of attachment is the femur or the tibia. Consequently, the length of the ACL varies from its anterior aspect to its posterior aspect wherein the posterior bundle is shorter than the anterior bundle [35]. This causes the posterior bundle to suffer a greater strain than the anterior bundle during a tibial translation movement, thereby making the posterior bundle more vulnerable to rupture [11, 57].

A number of knee morphologic variables have been identified as risk factors for ACL injury such as a small femoral notch, a higher-than-normal body-mass index (BMI), increased joint and ACL laxity, tibial plateau depth of cancavity, a steep posterior tibial slope, and variations in lower limb alignment [58-64]. McLean et al., 2011 demonstrated a significant association between the

posterior tibial slope and the anteromedial bundle ACL strain for dynamic high-impact jump landings [56]. Terauchi et al., 2011 summarized additional extrinsic factors such as shoe surface interaction, skill level, muscle strength and conditioning [54].

2.3 ACL repair and its outcomes

Because of the critical biomechanics role the ACL plays in knee function, abnormal kinematics caused by an ACL-deficient knee lead to further knee complications such as menisci tear, cartilage damage and eventually development of osteoarthritis. Therefore a surgical procedure to reconstruct the torn ACL using tendon grafts has been the standard procedure to repair a torn ACL. Despite the good outcomes, many limitations are also associated with the current ACL replacement methodology, such as donor site morbidity, graft availability, and mis-matched biomechanical properties between the graft and the native ACL.

2.3.1 Healing of the ligament

Tendons and ligaments that are composed of dense connective tissue heal the rupture site through a series of progressive events, namely inflammatory, proliferative, and remodeling phases [17]. As a result, a functional scar is formed at the wound bridging the rupture [17, 66]. Animal studies have shown that the MCL heals by bridging scar formation at the injury site. The healing process includes short phases of hemorrhage and inflammation, followed by a proliferation phase and then a prolonged remodeling phase [66, 67].

Unlike the MCL, the intra-articularly located ACL does not form the scar mentioned above. As previously discussed, in most ACL tear incidences, the tear occurs in the middle or proximal third portion of the ACL[68]. Histologic and immunohistochemistry analysis revealed that the cells within the ACL proliferate and migrate easily into the wound site, the ligament vascularizes after the tear, and collagen production recurs within the torn ACL [69 and the references within]. A layer of synovial tissue over the ruptured surface forms after the ACL

rupture occurs. This may hinder the ligament repair. A large number of myofibroblasts are differentiated in this synovial layer and in the epiligamentous tissue, which can cause the retraction of the ruptured ACL ends [17]. However, because of the anatomy and the function of the ACL, the ACL remnants pass each other in the knee joint and never reconnect. Thus it is impossible for the ACL to heal itself, regardless of the blood supply and cell activity they possessed [69].

Murray et al., 2000 described the four sequential phases of the ACL injury response in details. The key points of each phase are listed in Table 2.1 [17]. The authors pointed out that (1) the formation of a synovial layer that is abundant in cells expressing alpha-smooth muscle actin covers the surface of the rupture ends, (2) the lack of any scar tissue bridging the two ruptured ends, and (3) the presence of an epiligamentous reparative phase are the differences between the ACL response to rupture and responses of the other dense connective tissues to injury [17].

Table 2.1 Summary of the four sequential phases occurring after ACL rupture according to [17]

Phase	Time	Rupture site appearance	Cellular behavior	Vascularization
Inflammation	1- 2 weeks	1. no connection between the two ruptured ends 2. friable and stringy tissue that looks like "mop-ends"	1. fibroblasts populated the remnant 2. inflammatory cells: neutrophils and macrophages	1. dilated arteriols and venules 2. congested capillaries
Epiligamentous Regeneration	3 - 8 weeks	1. covered with gradually growing epiligamentous and synovial tissue 2. no tissue bridging the two ruptured ends 3. a synovial cell layer extending over the ruptured site surface	1. unchanged cell density in ACL 2. decreased number of inflammatory cells in ACL 3. increased cell density in epiligament	1. unchanged blood vessel density 2. no neovascularization in ACL 3. increased blood vessel density in epiligament
Proliferation	8 - 20 weeks	a complete synovial cell layer covering in the distal end	1. increased cell number density in the ACL with fibroblasts dominant 2. disorganized orientation of the fibroblasts in the ACL 3. abundant alpha-smooth muscle actin-containing cells in the synovial layer and throughout the ACL	increased blood vessel density in the ACL
Remodeling and Maturation	1 - 2 years	1. dense ACL remant with little fatty synovial tssue covering the surface 2. epiligamentous tissue covering the ACL remnant decreases in thickness	1. fibroblasts with nuclei aligned with the collagen fiber in ACL 2. cell density in the ACL found to be similar to the intact ACL	decreased blood vessel density in the ACL

In recent years, ACL rupture in children and adolescents is on the rise. The long-term consequences from an ACL-deficient knee are found to be more significant in younger and more active individuals (details can be found in [70]). Therefore, early reconstruction of an ACL-ruptured knee is thought to decrease subsequent cartilage and meniscal injury. Because the current ACL reconstruction techniques involve drilling across the physeal plates of both the femur and tibia, treatments to children and adolescents have been complicated. These skeletally immature patients have wide-open physes; hence, damage to the physes has been a significant concern using the current drilling techniques. This is because one may face severe consequences such as growth abnormalities. Physicians often face a dilemma in treating an ACL injury in a skeletally immature patient [70]. On one hand, these young patients are often active in sports and thereby at increased risk for suffering further intra-articular component damage; alternatively, a reconstruction increases risk of the development of growth abnormalities in the knee [70]. Therefore, the ideal treatment of these individuals is currently not clear.

Non-anatomic physeal-sparing surgical techniques are used to address the needs of skeletally immature patients [70] with the goal of avoiding bone tunnel passing through the physis during reconstruction. Concerns are raised in this technique because of the non-anatomic placement of the graft that could potentially cause abnormal knee loading. Physicians have also used the standard transphyseal reconstruction techniques in these patients with the goal of providing maximal knee stability while hoping to not disturb the growth plates of the young patient [70]. Some modifications from adult ACL reconstruction have been made including drilling smaller tunnels, lightly packing tunnels with a soft-tissue graft, and avoiding crossing physis with bone plugs or fixation devices [73]. Various grafts are used to perform the ACL reconstruction including hamstring autograft, iliotibial band grafts, patellar tendon grafts and quadriceps grafts [70].

2.3.2 Current surgical strategies

Clinicians believe that ACL reconstruction surgeries provide additional knee stability and potentially protect other components within the joint. Earlier surgery applying suture repair to bridge the ACL remnants failed to reconstruct the torn ACL [69]. The reconstruction using a graft to replace the torn ACL is currently the universal solution to treat the torn ACL. ACL injuries occur frequently and have a substantial financial cost. [71]. The most commonly used grafts in ACL reconstructions are patellar tendons, hamstring tendons and quadriceps tendons [72]. Autografts are the current gold standard for ACL replacements and the patellar tendon is the most common source of autograft tissue.

2.3.3 Outcomes of the current ACL reconstruction

The current treatment allows patients to return to rigorous activities in the vast majority of cases. A recent study reviewed 5770 patients who were athletes before ACL injury with a mean follow-up of 41.5 months and concluded that the ACL reconstruction has an overall high rate of successful outcomes based on the fact that about 90% of participants regained normal or nearly normal knee function (laxity and strength) [74]. However, only 63% of the participants returned to their pre-injury level of activity [74]. Despite the functional outcomes from the current surgical treatment, long-term results are not satisfactory. Other studies showed that many grafts function as mechanical springs that span the gap between the femur and tibia, providing initial stability and allowing joint motion, but do not complete the ligamentization process nor restore the original biomechanics to the knee even 2-3 years after surgery [26, 75]. Besides high economic cost, many limitations are associated with the current treatment. Specifically, autografts may result in surgical site morbidities and require a second surgery and possibly longer surgical procedure. Allografts carry the risk of transmitted diseases, are limited by donor availability, and may result in an immune rejection. Both graft types suffer mis-matched biomechanical properties. [45, 46, 75-79]. Using patellar tendon grafts, the most commonly used ACL graft,

as an example, its viscoelastic properties differ in several important ways from those of the ACL [80]: (1) the initial stiffness of the patellar tendon exceeds that of the ACL [81, 82], (2) the patellar tendon strain to failure at a given strain rate is significantly less than that of ACL, which may lead to increased failure incidences [81, 82], and (3) the patellar tendon failure strain is more sensitive to strain rate than the ACL failure strain; at higher strain rates the failure strain for the patellar tendon decreases rapidly [81], again leading to increased failure risks under impact loads. The mismatch may be critical in the generation of increased intra-articular forces, the early onset of osteoarthritis (OA) and high failure rates (20%) in young, active patients [70, 83, 84], and the risk of OA development [75, 77, 78, 85]. In addition, the incidence of early-onset OA within 7-14 years after knee injury is as high as 50% [78, 79, 86], without improved outcomes as a result of ACL reconstruction [78, 83].

A recent review demonstrated a high incidence of meniscal tears in this young group of patients who had ACL reconstructions. The authors concluded that this trend may be the result of the failure of physicians and parents of young patients to limit their physical activity as they wait for their skeleton to reach maturity [70]. Kocher et al., 2002 reported the increase in the incidence of growth disturbances in skeletally immature patients with ACL reconstructions [87]. In order to achieve successful reconstruction in this group, one must avoid trauma to the tibial apophysis. Another recent study reported that the combined injuries of ACL tears with cartilage or meniscal injury resulted in the highest incidence of long-term osteoarthritis [88].

To overcome the limitations of tendon auto- and allografts, synthetic polymer devices have been attempted as replacements of the torn ACL. These devices include Leeds-Keio ligament (Poly-ethylene terephthalate), Kennedy ligament augmentation device (polypropylene) and Gore-Tex (tetrafluoroethylene) [89]. These synthetic devices initially have sufficient mechanical stiffness. However, they all failed over time because they could not

meet the biomechanical requirements of the ligament [89]. One reason for the failure might be that the cells are not attracted to the synthetic device. Therefore, no extracellular matrix is produced in these devices. Thus, there is a need for a ligament graft that will develop biochemically relevant and biomechanically compatible interfaces with native tissue and restore the proper biomechanics and physiological function to the ligament. These limitations have led investigators to develop strategies to engineer ligament tissue to reduce or eliminate the need for graft tissue altogether [90]. Tissue engineering provides opportunities for a paradigm shift in the treatment for a torn ACL. In recent decades, investigators have been focusing on tissue engineering ACL grafts to improve the outcomes of the ACL repair. Most cellular based approaches utilize scaffolds (biologic materials, biodegradable materials or composites) with or without cells seeded to replace ACLs [90, 91].

2.4 Summary

The ACL has a complex anatomic structure which sustains the important function of the ACL in the knee joint including anterior tibial translation. Though ACL tears are commonly sustained during athletic activities by patients all ages; in recent years, the patient age at injury occurrence has declined for ACL tears. An ACL-deficient knee will induce other knee complications such as cartilage damage and meniscus tears, and eventually, osteoarthritis development. Tendon auto- or allografts are the current treatment standard to replace the torn ACL and restore normal knee function. Despite the favorable outcomes of the current reconstruction strategy, many well-known limitations are also associated with it, such as graft availability, risk of immune rejection, and mis-matched biomechanical properties between the graft and the native ACL it is meant to replace. These limitations have motivated researchers to investigate the development of a tissue engineered graft that can overcome these limitations and effectively replace the ACL.

2.5 References

1. Danylchuk, K.E.N.D., J.B. Finlay, and J.P. Krcek, *Microstructural organization of human and bovine cruciate ligaments.* Clinical orthopaedics and related research, 1978. **131**: p. 294.

2. Duthon, V.B., et al., *Anatomy of the anterior cruciate ligament.* Knee Surgery, Sports Traumatology, Arthroscopy, 2005. **14**(3): p. 204-213.

3. Hara, K., et al., *Anatomy of Normal Human Anterior Cruciate Ligament Attachments Evaluated by Divided Small Bundles.* The American Journal of Sports Medicine, 2009. **37**(12): p. 2386-2391.

4. Girgis, F.G., J.L. Marshall, and A. Monajem, *The cruciate ligaments of the knee joint. Anatomical, functional and experimental analysis.* Clinical orthopaedics and related research, 1975. **106**: p. 216-231.

5. Amis, A.A. and G.P. Dawkins, *Functional anatomy of the anterior cruciate ligament. Fibre bundle actions related to ligament replacements and injuries.* The Journal of Bone and Joint Surgery, 1991. **73**(2): p. 260-267.

6. Arnoczky, S.P., *Anatomy of the anterior cruciate ligament.* Clinical orthopaedics and related research, 1983. **172**: p. 19-25.

7. Chhabra, A., et al., *Anatomic, radiographic, biomechanical, and kinematic evaluation of the anterior cruciate ligament and its two functional bundles.* The Journal of Bone and Joint Surgery (American), 2006. **88 Suppl 4**: p. 2-10.

8. Norwood, L.A. and M.J. Cross, *Anterior cruciate ligament: functional anatomy of its bundles in rotatory instabilities.* The American Journal of Sports Medicine, 1979. **7**(1): p. 23-26.

9. Steckel, H., et al., *2D and 3D 3-tesla magnetic resonance imaging of the double bundle structure in anterior cruciate ligament anatomy.* Knee Surgery, Sports Traumatology, Arthroscopy, 2006. **14**(11): p. 1151-1158.

10. Rosenberg, T.D. and G.L. Rasmussen, *The function of the anterior cruciate ligament during anterior drawer and Lachman's testing. An in vivo analysis in normal knees.* The American Journal of Sports Medicine, 1984. **12**(4): p. 318-22.

11. Butler, D.L., et al., *Location-dependent variations in the material properties of the anterior cruciate ligament.* Journal of Biomechanics, 1992. **25**(5): p. 511-518.

12. Butler, D.L., M.D. Kay, and D.C. Stouffer, *Comparison of Material Properties in Fascicle-Bone Units From Human Patellar Tendon and Knee Ligaments.* Journal of Biomechanics, 1986. **19**(6): p. 425-432.

13. Steckel, H., et al., *Arthroscopic evaluation of the ACL double bundle structure.* Knee Surgery, Sports Traumatology, Arthroscopy, 2009. **17**(7): p. 782-785.

14. Ferretti, M., et al., *The fetal anterior cruciate ligament: an Anatomic and histologic study.* Arthroscopy: The Journal of Arthroscopic & Related Surgery, 2007. **23**(3): p. 278-283.

15. Hollis, J.M., S. Takai, and S.L. Woo, *The effects of knee motion and external loading on the length of the anterior cruciate ligament (ACL): a kinematic study.* Journal of Biomechanical Engineering, 1991. **113**(2): p. 208-214.

16. Petersen, W. and B. Tillmann, *Structure and vascularization of the cruciate ligaments of the human knee joint.* Anatomy and embryology, 1999. **200**(3): p. 325-334.

17. Murray, M.M., et al., *Histological changes in the human anterior cruciate ligament after rupture.* The Journal of Bone and Joint Surgery (American), 2000. **82-A**(10): p. 1387-1397.

18. Strocchi, R., et al., *The human anterior cruciate ligament: histological and ultrastructural observations.* Journal of Anatomy, 1992. **181 (Pt 3)**: p. 521-522.

19. Baek, G.H., et al., *Quantitative analysis of collagen fibrils of human cruciate and meniscofemoral ligaments.* Clinical orthopaedics and related research, 1998. **357**: p. 205-211.

20. Benjamin, M. and J.R. Ralphs, *Fibrocartilage in tendons and ligaments--an adaptation to compressive load.* Journal of Anatomy, 1998. **193 (Pt 4)**: p. 481-494.

21. Benjamin, M., et al., *Where tendons and ligaments meet bone: attachment sites (entheses) in relation to exercise and/or mechanical load.* Journal of Anatomy, 2006. **208**(4): p. 471-490.

22. Francois, R.J., J. Braun, and M.A. Khan, *Entheses and enthesitis: a histopathologic review and relevance to spondyloarthritides.* Current opinion in rheumatology, 2001. **13**(4): p. 255-264.

23. Ralphs, J.R., et al., *Regional differences in cell shape and gap junction expression in rat Achilles tendon: relation to fibrocartilage differentiation.* Journal of Anatomy, 1998. **193 (Pt 2)**: p. 215-22.

24. Waggett, A.D., et al., *Characterization of collagens and proteoglycans at the insertion of the human Achilles tendon.* Matrix biology : journal of the International Society for Matrix Biology, 1998. **16**(8): p. 457-70.

25. Wang, I.N.E., et al., *Age-dependent changes in matrix composition and organization at the ligament-to-bone insertion.* Journal of Orthopaedic Research, 2006. **24**(8): p. 1745-1755.

26. Moffat, K.L., et al., *Characterization of the structure-function relationship at the ligament-to-bone interface.* Proceedings of the National Academy of Sciences of the United States of America, 2008. **105**(23): p. 7947-7952.

27. Kennedy, J.C., H.W. Weinberg, and A.S. Wilson, *Anatomy and Function of Anterior Cruciate Ligament - as Determined by Clinical and Morphological Studies.* Journal of Bone and Joint Surgery-American Volume, 1974. **A 56**(2): p. 223-235.

28. Schutte, M.J., et al., *Neural anatomy of the human anterior cruciate ligament.* The Journal of Bone and Joint Surgery (American), 1987. **69**(2): p. 243.

29. Wojtys, E.M. and L.J. Huston, *Neuromuscular performance in normal and anterior cruciate ligament-deficient lower extremities.* The American Journal of Sports Medicine, 1994. **22**(1): p. 89.

30. Konishi, Y., T. Fukubayashi, and D. Takeshita, *Possible mechanism of quadriceps femoris weakness in patients with ruptured anterior cruciate ligament.* Medicine and science in sports and exercise, 2002. **34**(9): p. 1414-8.

31. Krogsgaard, M.R., P. Dyhre-Poulsen, and T. Fischer-Rasmussen, *Cruciate ligament reflexes.* Journal of electromyography and kinesiology : official journal of the International Society of Electrophysiological Kinesiology, 2002. **12**(3): p. 177-82.

32. Butler, D.L., *Anterior cruciate ligament: Its normal response and replacement.* Journal of Orthopaedic Research, 1989. **7**(6): p. 910-921.

33. Butler, D.L., *Anterior cruciate ligament: Its normal response and replacement.* Journal of Orthopaedic Research, 1989(7): p. 910-921.

34. Helfzy, M.e.a., *ACL intra-articular reconstruction: Factors affecting the region of most isometric attachments.* transactions of the 33rd annual meeting of the orthopaedic research society, 1987.

35. Amis, A.A., *The functions of the fibre bundles of the anterior cruciate ligament in anterior drawer, rotational laxity and the pivot shift.* Knee surgery, sports traumatology, arthroscopy, 2012. **20**(4): p. 613-620.

36. Zantop, T., W. Petersen, and F.H. Fu, *Anatomy of the anterior cruciate ligament.* Operative techniques in orthopaedics, 2005. **15**(1): p. 20-28.

37. Noyes, F.R. and E.S. Grood, *Strength of Anterior Cruciate Ligament in Humans and Rhesus-Monkeys.* Journal of Bone and Joint Surgery-American Volume, 1976. **58**(8): p. 1074-1082.

38. Woo, S.L., et al., *Tensile properties of the human femur-anterior cruciate ligament-tibia complex. The effects of specimen age and orientation.* The American Journal of Sports Medicine, 1991. **19**(3): p. 217-25.

39. Jones, R.S., et al., *Mechanical properties of the human anterior cruciate ligament.* Clinical Biomechanics, 1995. **10**(7): p. 339-344.

40. Chandrashekar, N., et al., *Sex-based differences in the tensile properties of the human anterior cruciate ligament.* Journal of Biomechanics, 2006. **39**(16): p. 2943-50.

41. Paschos, N.K., et al., *Cadaveric study of anterior cruciate ligament failure patterns under uniaxial tension along the ligament.* Arthroscopy : The Journal of Arthroscopic & Related Surgery : Official Publication of the Arthroscopy Association of North America and the International Arthroscopy Association, 2010. **26**(7): p. 957-67.

42. Azangwe, G., K.J. Mathias, and D. Marshall, *Preliminary comparison of the rupture of human and rabbit anterior cruciate ligaments.* Clinical Biomechanics, 2001. **16**(10): p. 913-917.

43. Woo, S.L.Y., et al., *Biomechanics of knee ligaments.* The American Journal of Sports Medicine, 1999. **27**(4): p. 533.

44. Orthopaedic, T.A.O.S.f.S.M.C.o.A.i., *Sports Medicine. Keystone (CO), July 14–17.* 2005.

45. Louw, Q.A., J. Manilall, and K.A. Grimmer, *Epidemiology of knee injuries among adolescents: a systematic review.* British Journal of Sports Medicine, 2008. **42**(1): p. 2-10.

46. Ingram, J.G., et al., *Epidemiology of knee injuries among boys and girls in US high school athletics.* The American Journal of Sports Medicine, 2008. **36**(6): p. 1116-22.

47. Frank, C.B. and D.W. Jackson, *The science of reconstruction of the anterior cruciate ligament.* The Journal of Bone and Joint Surgery (American), 1997. **79**(10): p. 1556-1576.

48. Busch, M.T., M.D. Fernandez, and C. Aarons, *Partial Tears of the Anterior Cruciate Ligament in Children and Adolescents.* CSM, 2011. **30**(4): p. 743-750.

49. Sonnery-Cottet, B., et al., *Arthroscopic Identification of Isolated Tear of the Posterolateral Bundle of the Anterior Cruciate Ligament.* YJARS, 2009. **25**(7): p. 728-732.

50. Ochi, M., et al., *Anterior Cruciate Ligament Augmentation Procedure With a 1-incision Technique: Anteromedial Bundle or Posterolateral Bundle Reconstruction.* Arthroscopy: The Journal of Arthroscopic & Related Surgery, 2006. **22**(4): p. 463.e1-463.e5.

51. Bach, J.M., M.L. Hull, and H.A. Patterson, *Direct measurement of strain in the posterolateral bundle of the anterior cruciate ligament.* Journal of Biomechanics, 1997. **30**(3): p. 281-283.

52. Griffin, L.Y., et al., *Noncontact anterior cruciate ligament injuries: risk factors and prevention strategies.* The Journal of the American Academy of Orthopaedic Surgeons, 2000. **8**(3): p. 141-50.

53. DeMorat, G., et al., *Aggressive quadriceps loading can induce noncontact anterior cruciate ligament injury.* American Journal of Sports Medicine, 2004. **32**(2): p. 477-483.

54. Terauchi, M., et al., *Sagittal alignment of the knee and its relationship to noncontact anterior cruciate ligament injuries.* The American Journal of Sports Medicine, 2011. **39**(5): p. 1090-1094.

55. McLean, S.G., et al., *Sagittal plane biomechanics cannot injure the ACL during sidestep cutting.* Clinical Biomechanics, 2004. **19**(8): p. 828-38.

56. McLean, S.G., et al., *The relationship between anterior tibial acceleration, tibial slope, and ACL strain during a simulated jump landing task.* The Journal of bone and joint surgery. American volume, 2011. **93**(14): p. 1310-7.

57. Robinson, J.R., A.M.J. Bull, and A.A. Amis, *Structural properties of the medial collateral ligament complex of the human knee.* Journal of Biomechanics, 2005. **38**(5): p. 1067-1074.

58. Nguyen, A.D. and S.J. Shultz, *Sex differences in clinical measures of lower extremity alignment.* Journal of Orthopaedic & Sports Physical Therapy, 2007. **37**(7): p. 389-398.

59. Braten, M., T. Terjesen, and I. Rossvoll, *Femoral Anteversion in Normal Adults - Ultrasound Measurements in 50 Men and 50 Women.* Acta Orthopaedica Scandinavica, 1992. **63**(1): p. 29-32.

60. Uhorchak, J.M., et al., *Risk factors associated with noncontact injury of the anterior cruciate ligament - A prospective four-year evaluation of 859 West Point cadets.* American Journal of Sports Medicine, 2003. **31**(6): p. 831-842.

61. Pflum, M.A., et al., *Model prediction of anterior cruciate ligament force during drop-landings.* Medicine and science in sports and exercise, 2004. **36**(11): p. 1949-1958.

62. Hashemi, J., et al., *The Geometry of the Tibial Plateau and Its Influence on the Biomechanics of the Tibiofemoral Joint.* Journal of Bone and Joint Surgery-American Volume, 2008. **90A**(12): p. 2724-2734.

63. Boden, B.P., I. Breit, and F.T. Sheehan, *Tibiofemoral Alignment: Contributing Factors to Noncontact Anterior Cruciate Ligament Injury.* Journal of Bone and Joint Surgery-American Volume, 2009. **91A**(10): p. 2381-2389.

64. McLean, S.G., et al., *Knee joint anatomy predicts high-risk in vivo dynamic landing knee biomechanics.* Clinical Biomechanics, 2010. **25**(8): p. 781-788.

65. Zantop, T., et al., *Intraarticular rupture pattern of the ACL.* Clinical orthopaedics and related research, 2007. **454**: p. 48-53.

66. Frank, C., N. Schachar, and D. Dittrich, *Natural history of healing in the repaired medial collateral ligament.* Journal of Orthopaedic Research, 1983. **1**(2): p. 179-188.

67. Abramowitch, S.D., et al., *A biomechanical and histological evaluation of the structure and function of the healing medial collateral ligament in a goat model.* Knee Surgery, Sports Traumatology, Arthroscopy, 2003. **11**(3): p. 155-162.

68. Sherman, M.F., et al., *The long-term follow-up of primary anterior cruciate ligament repair - defining a rationale for augmentation.* American Journal of Sports Medicine, 1991. **19**(3): p. 243-255.

69. Murray, M.M., *Current Status and Potential of Primary ACL Repair.* Clinics in Sports Medicine, 2009. **28**(1): p. 51-61.

70. Kaeding, C.C., D. Flanigan, and C. Donaldson, *Surgical Techniques and Outcomes After Anterior Cruciate Ligament Reconstruction in Preadolescent Patients.* Arthroscopy : The Journal of Arthroscopic & Related Surgery : Official Publication of the Arthroscopy Association of North America and the International Arthroscopy Association, 2010. **26**(11): p. 1530-1538.

71. Statistics, N.C.f.H., *National Ambulatory Medical Care Survey.* Available on the American Association of Orthopaedic Surgeons web page at aaos.org., 2004.

72. Leal-Blanquet, J., et al., *Anterior cruciate ligament reconstruction: a multicenter prospective cohort study evaluating 3 different grafts using same bone drilling method.* Clinical journal of sport medicine : official journal of the Canadian Academy of Sport Medicine, 2011. **21**(4): p. 294-300.

73. Simonian, P.T., M.H. Metcalf, and R.V. Larson, *Anterior cruciate ligament injuries in the skeletally immature patient.* American journal of orthopedics, 1999. **28**(11): p. 624-8.

74. Ardern, C.L., et al., *Return to sport following anterior cruciate ligament reconstruction surgery: a systematic review and meta-analysis of the state of play.* British Journal of Sports Medicine, 2011. **45**(7): p. 596-606.

75. Scheffler, S.U., F.N. Unterhauser, and A. Weiler, *Graft remodeling and ligamentization after cruciate ligament reconstruction.* Knee Surgery, Sports Traumatology, Arthroscopy, 2008. **16**(9): p. 834-842.

76. Alhadlaq, A. and J.J. Mao, *Mesenchymal stem cells: isolation and therapeutics.* Stem cells and development, 2004. **13**(4): p. 436-448.

77. Salgado, A.J., O.P. Coutinho, and R.L. Reis, *Bone tissue engineering: state of the art and future trends.* Macromolecular bioscience, 2004. **4**(8): p. 743-65.

78. Roos, E.M., *Joint injury causes knee osteoarthritis in young adults.* Current opinion in rheumatology, 2005. **17**(2): p. 195-200.

79. von Porat, A., E.M. Roos, and H. Roos, *High prevalence of osteoarthritis 14 years after an anterior cruciate ligament tear in male soccer players: a study of radiographic and patient relevant outcomes.* Annals of the rheumatic diseases, 2004. **63**(3): p. 269-73.

80. Ma, J., et al., *Three-dimensional engineered bone-ligament-bone constructs for anterior cruciate ligament replacement.* Tissue engineering.Part A, 2012. **18**(1-2): p. 103-116.

81. Danto, M.I. and S.L. Woo, *The mechanical properties of skeletally mature rabbit anterior cruciate ligament and patellar tendon over a range of strain rates.* Journal of orthopaedic research : official publication of the Orthopaedic Research Society, 1993. **11**(1): p. 58-67.

82. Chandrashekar, N., et al., *Low-load behaviour of the patellar tendon graft and its relevance to the biomechanics of the reconstructed knee.* Clinical Biomechanics, 2008. **23**(7): p. 918-25.

83. Lohmander, L.S., et al., *High prevalence of knee osteoarthritis, pain, and functional limitations in female soccer players twelve years after anterior cruciate ligament injury.* Arthritis and rheumatism, 2004. **50**(10): p. 3145-52.

84. Spindler, K.P. and R.W. Wright, *Clinical practice. Anterior cruciate ligament tear.* The New England journal of medicine, 2008. **359**(20): p. 2135-42.

85. Wilder, F.V., et al., *History of acute knee injury and osteoarthritis of the knee: a prospective epidemiological assessment. The Clearwater Osteoarthritis Study.* Osteoarthritis and cartilage / OARS, Osteoarthritis Research Society, 2002. **10**(8): p. 611-6.

86. Kessler, M.A., et al., *Function, osteoarthritis and activity after ACL-rupture: 11 years follow-up results of conservative versus reconstructive treatment.* Knee surgery, sports traumatology, arthroscopy : official journal of the ESSKA, 2008. **16**(5): p. 442-8.

87. Kocher, M.S., et al., *Management and complications of anterior cruciate ligament injuries in skeletally immature patients: survey of the Herodicus Society and The ACL Study Group.* Journal of pediatric orthopedics, 2002. **22**(4): p. 452-7.

88. Oiestad, B.E., et al., *Knee Osteoarthritis After Anterior Cruciate Ligament Injury A Systematic Review.* American Journal of Sports Medicine, 2009. **37**(7): p. 1434-1443.

89. Laurencin, C.T. and J.W. Freeman, *Ligament tissue engineering: an evolutionary materials science approach.* Biomaterials, 2005. **26**(36): p. 7530-7536.

90. Petrigliano, F.A., D.R. McAllister, and B.M. Wu, *Tissue engineering for anterior cruciate ligament reconstruction: a review of current strategies.* Arthroscopy : The Journal of Arthroscopic & Related Surgery : Official Publication of the Arthroscopy Association of North America and the International Arthroscopy Association, 2006. **22**(4): p. 441-451.

91. Ge, Z., et al., *Biomaterials and scaffolds for ligament tissue engineering.* Journal of biomedical materials research.Part A, 2006. **77**(3): p. 639-652.

92. http://www.drugs.com/health-guide/acl-anterior-cruciate-ligament-injuries.html

93. http://www.omnipt.net/media/img/21/ankle_anatomy_tendons01.jpg

94. Scranton P.E., et al., *Mechanisms of anterior cruciate ligament neovascularization and ligamentization*, Arthroscopy: The Journal of Arthroscopic and Related Surgery, 1998. **14**(7): p. 702-716

CHAPTER 3

Scaffold-Less Tissue Engineered Bone-Ligament-Bone Constructs

Tissue engineering provides opportunities for a paradigm shift in the treatment of a torn ACL. For the past decades, investigators have attempted to find tissue engineered ACL grafts with biomechanical properties similar to the native ACL. Current tissue engineering methodologies utilize various biocompatible scaffolds, fibroblast or mesenchymal stem cells, and growth factors that promote cell proliferation and differentiation to engineer grafts *in vitro*. While tissue engineered scaffolds have many advantages, limitations such as undesirable degradation rates of the scaffolds, immediate cell death after implantation, and mis-matched biomechanical properties hinder their ability to develop into a mature tissue that can replace the native ACL.

For these reasons, we have developed a compliant, scaffold-less tissue engineered construct using bone marrow stromal cells. The efficacy of this scaffold-less cell-based approach was demonstrated via morphological and mechanical analyses using a bone-ligament-bone construct (BLB) in a rat medial collateral ligament replacement. The approach was then used to replace the ACL in a sheep model. After two months of *in vivo* recovery, a functional enthesis was generated between the tissue engineered construct and the native tissue. Vascularization and innervation development were found as early as three months *in vivo*. By six months of *in vivo* recovery, the morphology of collagen and collagen fascicles matched the native ACL longitudinally and cross-sectionally. By nine months of *in vivo* recovery, the morphological properties and biomechanical properties (to be discussed in **Chapter 4**) were superior to those of the patellar tendon autograft, the commonly used tendon graft for ACL repair.

These results suggest that this scaffold-less tissue engineering technique is promising for ACL repair.

3.1 Current trends in tissue engineering

Current tissue engineering approaches utilize (1) scaffolds that promote tissue regeneration, (2) isolated cells that continuously proliferate and differentiate in vitro, (3) growth factors that facilitate *in vitro* or *in vivo* tissue regeneration, or (4) combinations of the elements enumerated above [1-6]. The incorporation of growth factors has been used to enhance cell migration, proliferation, and collagen deposition in ACL repair. Issues currently hindering clinical use of engineered tendons and ligaments include mechanical properties of the engineered graft that shield cells and inhibit neoligamentous tissue growth, challenges associated with integration between host bone and newly developed tissue and a rapid rate of scaffold degradation *in vivo* with a corresponding rate of tissue regeneration that is too slow [7].

3.1.1 Scaffold

Current tissue engineering approaches usually involve seeding cells onto natural or synthetic scaffolds that are both biocompatible and biodegradable [4]. Ideally, scaffolds should be capable of: (1) bridging complex three-dimensional (3D) anatomical defects; (2) facilitating tissue regeneration by promoting embedded cell adhesion, migration, and proliferation; (3) providing temporary mechanical support until the generation of the neotissue reaches a self-sustaining state; and (4) biodegrading with a degradation rate compatible with the rate of the neotissue formation [2]. Typically the scaffold, initially mimicking the structural and mechanical properties of the ACL, gradually degrades and transfers the mechanical loads to the new tissue regenerated within the scaffold. The current paradigm is to match or exceed native ligament stiffness and strength in order to restore stability to the knee [8]. Both biological and synthetic materials have been investigated as potential scaffold materials for tissue-engineered knee ligament repair, including collagen, silk, biodegradable polymers and composite materials, all with limited success [3, 8]. Knitting,

braiding, and electrospinning are popular techniques used in the manufacture of biocompatible fibrous scaffolds for ligament tissue engineering. Biological materials used in tissue engineering ligament are the common biological components of the extracellular matrix such as collagens and proteoglycans. Biologically derived materials naturally contain information that facilitates cell attachment and function and it is believed that these signals from biologically derived extracellular matrix materials may continue to provide stimuli to provide guidance to tissue remodeling [9]. Synthetic materials are easy to fabricate and store. They also have good mechanical strength. Therefore, a combination of the two may provide the most optimal solution by synergizing the advantages from both types of materials [10].

Dunn et al., 1992 fabricated an ACL graft by embedding aligned cross-linked collagen fibers in collagen matrix. The graft was used to replace the ACL in a rabbit model. The study demonstrated neotissue formation after 20 weeks post-operation (PO). The resorbable scaffold initially weakened (4 weeks PO). The scaffold gained a higher ultimate tensile strength at 20 weeks PO compared to the 4 weeks PO and the initial ultimate tensile strength prior to surgery because of the ingrowth and remodeling of neotissue at 20 weeks PO [10]. The authors concluded that the composite graft encouraged the development of functional neoligament tissue [10]. Cavallaro et al., 1994 extracted type I collagen from bovine tendons and used a collagen threadmaking apparatus to fabricate the collagen threads [9]. The apparatus extruded the collagen into a buffered solution of polyethylene glycol, followed by rinsing and air-drying. The threads were crosslinked and knitted to form a collagen fabric that provided a highly ordered structure with high ultimate tensile strength. The collagen fabric was then used to replace the ACL in a dog model. The TEM analysis showed that the neoligament in the mid-substance of the graft at 12 weeks PO was not as well organized as the native tissue, but the fibril diameter distribution pattern of the graft was found to be similar to that of the native ACL. No mechanical analysis was reported in this study and thus made it difficult to evaluate the mechanical

properties of the grafts [9]. Altman et al., 2002 developed a twisted fibrous silk matrix that consisted of bundles of silk fibers [11]. Their *in vitro* work has shown that the silk scaffold promotes cell proliferation and its mechanical properties, including ultimate load to failure, geometric stiffness, and elongation to failure, are similar to those of the native ACL [11]. Li et al., 2007 designed an electrospun scaffold fabrication method to fabricate an anisotropic biodegradable nanofibrous scaffold, composed of poly-ε-capeolaxrone, for tissue engineering applications. The anisotropy and mechanical properties such as Young's modulus, yield strain, and stress can be controlled in this method [12]. Freeman et al., 2011 has investigated combining a novel poly L-lactic acid (PLLA) fibrous scaffold with a poly diacrylate PLLA hydrogel for ACL tissue engineering *in vitro*. The PLLA fibrous scaffold graft provided a similar stress-strain response as that of the native ACL. Hydrogel absorbs water and releases it during stretch. Therefore, the addition of the hydrogel enhanced the viscoelasticity of the graft [13]. Cooper et al., 2007 developed synthetic braided PLLA scaffolds seeded with primary rabbit ACL cells as grafts for ACL repair in a rabbit model [14]. At 12-weeks PO, histological analysis demonstrated tissue healing and regeneration in the graft. The biomechanical degradation of the cell-seeded scaffold was not dramatically different from that of the control graft [14]. The tissue engineered approaches described above attempted to match the biomechanical properties of the native ACL by combining multiple synthetic structures and varying physical properties of these structures (e.g., density, braiding pattern and the number of crosslinks between fibers). However, unfavorable biomechanical degradation and instability occurs. The integration of the graft with native bone was not evident in most of these studies. Spalazzi et al., 2006 proposed a triphasic scaffold that consisted of three distinct but continuous regions to mimic the native ligament to bone insertion --ligament, ligament-bone interface, and bone. Phase 1 of the scaffold was made of polyglactin knitted mesh sheets; phase 2 was made of poly (D-L-lactide-co-glycolide) copolymer (PLGA) microspheres; phase 3 was made of composite microspheres consisting of PLGA and bioactive glass [18]. The scaffold was tri-

cultured with fibroblasts, chondrocytes, and osteoblasts and used as an ACL graft in a rat model. 8 weeks after *in vivo* recovery, the scaffold demonstrated that it facilitated multilineage cellular interactions, tissue infiltration, and abundant matrix production, thus presenting itself as a potential for regenerating the interface between soft tissue grafts and bone in tissue engineering ACL grafts [19]. The co-cultured scaffold degraded over time *in vivo* with a significantly decreased compressive modulus measured at 8 weeks PO as compared to the modulus obtained *in vitro*. The scaffold did however maintain the structural integrity required for endogenous tissue growth.

The use of acellularized tissue as ACL grafts has also become popular because of its advantages such as biomechanical stability, biocompatibility and improved ability for cellular repopulation and remodeling [15-17]. *In vitro* studies showed good biomechanical properties of the tendon allograft [15, 16]. However, *in vivo* results are more relevant to evaluating the efficacy of the graft. This source of this rationale is that only analyses from *in vivo* results demonstrate the long-term characteristics of the grafts such as the neotissue development and enthesis formation between the graft and native bone. Tischer et al., 2010 used acellularized semitendinosus tendon allografts with autologous fibroblasts and replaced the ACL in a rabbit model. The study demonstrated the overall inferior biomechanical properties of these cell seeded tendon allografts after 8 weeks PO. The geometric stiffness of these tendon allografts only attained 20% of that of the native ACL. The authors concluded that graft design modifications, such as acellularization process, must be performed in further studies to yield better *in vivo* results [17].

In conclusion, while scaffolding strategies appear to promote fibroblastic or osteogenic cell growth, undesirable characteristics such as a tendency to rupture, loss of stiffness and strength *in vivo*, immune rejection, improper scaffold degradation rates, and weak implant/native tissue interfaces have eliminated many scaffold-based tissue engineered ligament approaches from further

consideration [20]. The mechanical property requirements of engineered ligament at the time of replacement remain under debate [3, 8, 21]. The discussed tissue engineered scaffolds usually have higher material properties at the time of implantation. Recent evidence suggests that stiff scaffolds shield the cells within these structures from strains required for proper signal induction and hence, growth of neoligamentous tissue [3, 8, 20]. The result is loss of viability with time *in vivo* and increased joint laxity [20, 21]. Moreover, the stresses during normal anterior cruciate ligament (ACL) function do not typically exceed 20% of ACL strength [21], suggesting that current engineering approaches over-design for strength, especially if eventual collagen growth and remodeling are expected with time. The biomechanical mis-match and dissimilar tissue interface between native bone and engineered ligament are other existing design issues that may impede clinical applications [7, 22].

3.1.2 Cells

Ligament is composed of both fibroblasts and the extracellular matrix secreted by the fibroblasts. Attempts to mimic this environment by depositing cells onto scaffolds for tissue engineering applications has lead to contradictory results in previous studies by others in the field. While Tischer et al., 2010 showed a decrease in the biomechanical properties of scaffolds embedded with autologous fibroblasts 8 weeks PO [17], other studies showed that scaffolds embedded with fibroblasts or mesenchymal stem cells (MSCs) have greatly enhanced *in vivo* performances as compared to unseeded scaffolds, as previously described in Cooper et al., 2007 [14]. The optimal cell source for ligament tissue engineering is still under investigation. The variation in the behavior of cells from different cell sources, passage numbers, and the animal models all contribute to the consideration of cell selection [2]. Current cell-based tissue engineering approaches for ligament and tendon repair include primary fibroblasts derived from ligaments and tendons such as the ACL, medial collateral ligament (MCL), patellar tendon or Achilles tendon [23] or MSCs isolated from bone marrow stromal cells (BMSC) [24].

Given the proper environment, BMSCs can differentiate into many types of mesenchymal lineages including bone, ligament, tendon, cartilage, muscle, nerve and fat [25, 26]. BMSCs have demonstrated advantages over differentiated cells such as ACL fibroblasts that may render them optimal for ligament engineering, and their potential for tissue regeneration is the subject of ongoing investigations. BMSCs are capable of self-renewal and have more differentiation potential than fibroblasts originating from the ligament or tendon. Moreover, the proliferation system of BMSCs is robust and their adaptability to local environments (e.g. *in vitro* investigation) is strong [3, 27]. BMSCs create an environment that diminishes immune response and enhances regeneration. Thus the potential to use allogenic sources rather than autogenic sources of BMSC exists [28]. BMSCs can be isolated from autologous sources and may be expanded in culture while maintaining their multipotency which makes them an attractive candidate for tissue engineering [25, 28-32]. BMSCs also secrete bioactive factors that inhibit scarring and apoptosis and stimulate angiogenesis [28]. BMSCs are an accessible and biocompatible source of cells that are immunosuppressive, especially for T-cells [28], making both autogenic and allogenic sources good candidates for use in regenerative medicine.

Hairfield-Stein et al., 2007 used porcine BMSCs to generate self-organized rod-like tissues with silk suture segments as anchor points in a 14-day culturing period [33]. Fan et al., 2009 seeded MSC derived from bone marrow onto micro-porous silk scaffolds. Their *in vitro* study indicated that MSCs proliferated and differentiated into fibroblast-like cells. The cell-seeded graft was then used to replace the ACL in a pig model. After 24 weeks PO, the MSCs in the graft exhibited a fibroblast morphology. The scaffold survived *in vivo* 24 weeks PO with a significant amount of scaffold degradation. The enthesis zones were observed in these remodeled grafts [24].

3.1.3 Growth factors

Previous studies have shown the requirements for driving BMSCs to bone *in vitro* are ascorbic acid, dexamethasone (DEX), TGF-b, FGF-b, and an organic phosphate [34-40]. In contrast, BMSCs cultured in TGF-b, FGFb, and ascorbic acid in the absence of DEX can be driven to a ligament lineage [40-42]. In recent years, platelet-rich plasma (PRP) therapy has started to spread into many clinical applications including ACL repair. The method collects and concentrates autologous platelets to activate and release high concentration of the growth factors such as PDGF, TGF-beta, VEGF, FGF and EGF. Because of large amounts of growth factors it contains, the method has been used to stimulate tissue growth and regeneration clinically [43, 44]. Ascorbic acid is essential for hydroxyproline formation. Without hydroxyproline, the collagen triple helix cannot maintain its 3D conformation [72].

3.1.4 Morphological characterization methods of tissue engineered ligaments

Since a single specific marker does not exist for either bone or ligament, characterization of tissue types engineered from MSCs involves morphological observations of cellular and ECM structures and the presence of the expected cell biomarkers generally found in neonatal bone and ligament. For bone, the presence of alkaline phosphatase, an enzyme that cleaves phosphate ions from organic molecules, is a precursor to mineralization and thus an early sign of bone formation [45]. Type I collagen mineralized with hydroxyapatite crystals, the presence of osteocalcin, and the absence of type II collagen, the predominant protein of cartilage, are also used as markers of a bone lineage and have been shown to be characteristics of *in vitro* EBC from BMSCs [40]. In addition, RUNX2 is used to visualize pre-osteoblasts in the periosteum, osteoblasts and osteocytes in the bone, while CD31 is used to visualize the blood supply in the bone [46, 47]. Ligament lineage is characterized by type I collagen, the lack of mineralization, positive staining for elastin and negative staining for type II collagen.

3.1.5 Remarks

There are many advantages to current tissue engineering strategies with scaffolds including immediate stability [3, 48]. However, cellular stress-shielding can limit the ability of the cells within the scaffold to develop and replace the native ACL. In addition, the region of the graft or engineered material within the bone tunnel may not fully integrate with native tissue [49]. The initial response of the body to either grafts or current tissue engineering approaches results in reduced stiffness of the replacement [50]. The biomechanical mismatch and dissimilar tissue interface between native bone and engineered ligament are additional existing design limitations that may impede translation to clinical applications [7, 22].

Recently, our laboratory has successfully fabricated engineered ligament constructs (ELC) and engineered bone constructs (EBC), using these specific growth factors on BMSCs during proliferation and differentiation *in vitro* [40]. Furthermore, co-culturing these two types of constructs enabled us to generate 3D bone-ligament-bone (BLB) constructs with viable entheses *in vitro*. The use of the engineered BLB as a medial collateral ligament (MCL) or an ACL is discussed in the following sections.

3.2 Creation of a bone-ligament-bone (BLB) construct and its use as a medial collateral ligament (MCL) replacement

Because of the limitations current tissue engineering researchers are facing utilizing scaffolds, our laboratory has developed a compliant, co-cultured, and scaffold-less tissue engineered construct. In this approach, isolated bone marrow stromal cells (BMSC) are differentiated along osteogenic and fibrogenic pathways and in doing so, generate their own extra-cellular matrices. Cell contraction within the matrix leads to the formation of three dimensional constructs without artificial scaffolds. The engineered construct forms viable bone-ligament interfaces in vitro. Its efficacy as a ligament graft was demonstrated when used as an MCL replacement in the rat. The implanted BLB

not only possessed a large amount of viable cells, but also developed vascular and neural systems.

3.2.1 In vitro co-culture of BLB constructs

3.2.1.1 Preparation of solutions and media

Unless otherwise indicated, all solutions and media were prepared and stored at 4°C prior to the isolation and culture of cells and warmed to 37°C in a heated water bath immediately prior to use. The media, with slight modifications from [51, 52], were as follows: for ligament, growth medium (GM) consisted of 400 ml of Dulbecco's Modified Eagle Medium (DMEM; Gibco, Rockville, MD, Cat# 10565-042) with 100 ml Fetal Bovine Serum (FBS; Gibco, Rockville, MD, Cat# 10437-028), 6 μg/ml fibroblast growth factor basic (FGFb; Peprotech, Rocky Hill, NJ, Cat# 100-18B), 0.13 mg/ml asc-2-phos (Sigma, St. Louis, MO, Cat# A8960-5G), 0.05 mg/ml L-proline (Sigma, St. Louis, MO, Cat# P5607-25G), 5 ml antibiotic-antimycotic (Sigma, St. Louis, MO, Cat# A9909) and differentiation medium (DM) consisted of 460 ml DMEM with 35 ml 100% Horse Serum Albumin (HSA, Gibco, Rockville, MD, Cat# 16050-122), 0.13 mg/ml asc-2-phos, 0.05 mg/ml L-proline, 2 ng/ml transforming growth factor-beta (TGF-b; Peprotech, Rocky Hill, NJ, Cat# 100-21), and 5 ml antibiotic-antimycotic (Sigma, St. Louis, MO, Cat# A9909). For bone, the growth and differentiation media were the same as GM and DM, respectively, with the addition of 10^{-8} M dexamethasone (DEX; Sigma, St. Louis, MO, D4902-25MG).

3.2.1.2 Preparation of Culture Dishes

BLB constructs were engineered in individual 35 mm plates. Briefly, each 35 mm plate was coated with 1.5 ml of Sylgard (Dow Chemical Corporation, Midland, MI, type 184 silicon elastomer) and allowed to cure for 3 weeks prior to use. Sylgard coated plates were then coated with laminin at 3.0 $\mu g/cm^2$ per plate (30 μg of Natural Mouse Laminin (Gibco, Rockville, MD, Cat# 23017-015) and 3

ml of Dulbecco's Phosphate-Buffered Saline (DPBS) pH 7.2 (Gibco, Rockville, MD, Cat# 14190-144) per plate) and dried for 48 h. Salt crystals were dissolved and removed by rinsing the plates with 3 ml DPBS. The plates were then filled with 2 ml of previously described GM, decontaminated with UV light (wavelength 253.7 nm) for 90 minutes and placed in a 37°C, 5% CO_2 incubator for 1 week prior to plating BMSC.

3.2.1.3 Bone Marrow Stem Cell Isolation and Expansion

Surgical procedures were performed to remove both femurs for the isolation of bone marrow stromal cells (BMSC). The marrow was flushed from the donor bone tissue using a syringe with an 18½-gage needle filled with GM. The marrow was further dissociated by mixing with a 21½-gage needle before being centrifuged at 480 g for 5 minutes at 25°C. The pellet was resuspended in 10 ml GM (as appropriate for constructs under construction, ligament versus bone) and plated into 100 mm diameter tissue culture dishes. The dishes were kept in an incubator at 37 °C, 95% humidity, and 5% CO_2. After 48 h, the non-adherent cells were removed by rinsing with DPBS. The adherent BMSC were cultured to 80% confluence, at which time the cells were enzymatically removed from the 100 mm plates using a 0.25% trypsin-EDTA solution (Gibco, Rockville, MD, Cat# 25200-072) and passaged. Cells were plated onto prepared culture dishes within the third and fifth passages.

3.2.1.4 Preparation of Self-Organized Bone Constructs

After pre-incubation, the GM was aspirated and 2 * 10^5 cells per 35 mm dish were seeded onto each laminin-coated Sylgard plate, after which the bone GM was changed at 2–3 days. After approximately 3 days, when the cells became confluent, bone DM was substituted to induce construct formation. The DM was changed every 2–3 days until the constructs were ready to co-culture with ligament.

3.2.1.5 Bone-Ligament-Bone Construct Formation

The GM was aspirated from additional laminin-coated Sylgard plates and 2 ml of the ligament cell suspension containing 2 * 10^5 cells/ml-GM were plated in each 35 mm culture dish. The plates were maintained in a 37°C, 5% CO_2 incubator and the ligament GM was changed at 2-3 days. After the cells became confluent, approximately 3 days later, engineered bones (fabricated as described above) were cut into two segments and each segment was pinned using two minutien pins on top of the ligament cell monolayer such that the proximal bone construct ends were 10 mm apart. Following bone pinning, GM was replaced with ligament DM and this ligament DM was changed every 2-3 days. Approximately 1 week following the introduction of DM, the ligament monolayer rolled up around the bone construct forming a 3D BLB construct with a total length of 15 mm **(**Figure 3.1**A)**. All constructs were held in culture and fed fresh DM every 2-3 days for one week, at which point 6 constructs were used for medial collateral ligament (MCL) one-month replacement and 3 constructs were used for two-month replacement. The remaining constructs were held in culture an additional 4 weeks to serve as time matched controls for the *in vivo* studies. Of these 6 one-month explanted constructs, 2 were prepared for histological analysis and 4 for cyclic tension tests. All 3 two-month explanted constructs were prepared for histological analysis.

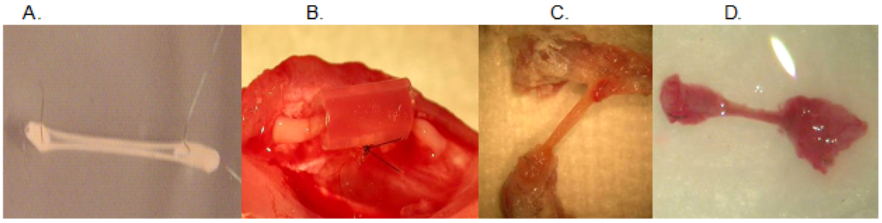

Figure 3.1 Fabrication, implantation, and explantation of 3D Bone-Ligament-Bone (BLB) constructs engineered *in vitro* for Medial Collateral Ligament Replacement. (A) BLB construct just prior to implantation; approximately 3 days after detachment of the monolayer, the cells self organized into a cylinder. Total length of the construct pin to pin = 15 mm; diameter = 0.47 mm. (B) 3D BLB from image (A) placed inside silicone tubing and secured in replacement of excised MCL; (C) 3D BLB construct four weeks following implantation. The presence of the silicone tubing makes it easy to visualize and excise the implanted construct; following one month of implantation, the engineered BLB has fused with the bone at the femur and tibia and increased in diameter to 0.53 mm. (D) 3D BLB excised from bone to be used for histology [53].

3.2.2 *In vivo* BLB construct implantation as an MCL replacement in rat

3.2.2.1 Animal Model and Animal Care

Female Fischer 344 rats obtained from the Charles River Laboratories, Inc. (Wilmington, MA) were used. All animals were acclimated to our colony conditions, i.e., light cycle and temperature, for 1 week prior to any procedure. Rats were housed in hanging plastic cages (28 × 56 cm) and maintained on a 12h/12h light/dark cycle at a temperature of 20-22°C. The animals were fed Purina Rodent Chow 5001 laboratory chow and were given free access to water. All surgical procedures were performed in an aseptic environment with animals in a deep plane of anesthesia induced by i.p. injections of sodium pentobarbital (50 mg/kg). Supplemental doses of pentobarbital were administered as required to maintain an adequate depth of anesthesia. Following any surgical procedure, the animals were singly housed until the date of explantation. All animal care and animal surgeries were in accordance with The Guide for Care and Use of Laboratory Animals (Public Health Service, 1996, NIH Publication No. 85-23); the experimental protocol was approved by the University Committee for the Use and Care of Animals.

3.2.2.2 MCL Replacement via Engineered BLB Constructs

Six BLB constructs fabricated from the isolated BMSCs were used as MCL replacements in host rats **(**Figure 3.1**B-D)**. The rat MCL replacement model was used because the size of the adult native rat MCL (12 mm x 3 mm) is approximately the same as that of our engineered BLB construct (15 mm x 0.47 mm). Additionally, the MCL is superficial, providing easy access to bone at the femur and the tibia, thus simplifying both the replacement of ligament and the recovery from the surgical procedures. Briefly, the distal medial head of the femur and proximal medial head of the tibia were exposed. The muscle and connective tissue surrounding the MCL were reflected exposing the MCL, which was severed from its points of insertions on both the femur and tibia. The native MCL was preserved for subsequent analysis of structure and function. A Dremel

drill was used to drill 0.9 mm holes at the points of MCL insertion on the femur and tibia. A portion of the ligament region of the engineered BLB construct was surrounded by a 1.6 mm ID diameter silicone tube for subsequent identification during explantation **(**Figure 3.1**B)**, and the bone sections of the construct were inserted into the drill holes. The constructs were secured to the bone by suturing them to the surrounding connective tissue. Finally, the muscle layers were closed using 7-0 suture and the skin was closed using 4-0 suture. Within one hour, animals were awake and resumed normal cage activities of eating and drinking. All animals were allowed to recover for either one or 2 months before removal of the BLB explants. Prior to surgery and following the recovery period and prior to construct explantation, all animals were assessed for locomotor function using foot print analysis and rotorod testing [54]. Either one or two months following the explantation, the entire knee was extracted from the animal **(**Figure 3.1**C)**, the engineered construct was isolated from surrounding tissues, and the patellar tendon, ACL, posterior cruciate ligament, and lateral collateral ligament were excised leaving the BLB-based MCL replacement tissue adhered to the femur and tibia (Figure 3.1**D**)**.** The explanted BLB constructs were either fixed for histochemical analysis or briefly placed in transfer media (DPBS with 2% antibiotics) prior to mechanical testing.

3.2.2.3 Native MCL Dissections

Pregnant Fischer 344 rats were obtained at 13 days into the gestation and acclimated under the same conditions as previously described. Fourteen days following the birth of the pups rats were euthanized with an overdose of sodium pentobarbital (100 mg/kg) administered by intraperitoneal injection. The legs were dissected, removing the skin and muscle but maintaining the ligament connections at the knee. The MCL (n=5) was isolated by removing all other knee ligaments. The tibia and femur were cut mid-bone to provide tissue for gripping during mechanical testing. Both MCLs were removed from the rat and fixed for histochemical analysis.

3.2.3 Morphological analysis of the BLB *in vitro*, BLB *explant*, and native MCLs

Histochemical and immunofluorescent staining was conducted to obtain the cell availability, the morphology of extracellular matrix, vascularization, and innervation of the BLB in vitro, BLB explant, and native MCLs. These samples were placed into TBS medium, frozen in cold isopentane and stored at -80^{0}C until needed.

For histochemical staining, three to five samples per group of 3D BLB constructs developed *in vitro* and after implantation *in vivo* and native MCLs were analyzed. Samples were sliced longitudinally with a cryostat at a thickness of approximately 12 μm, adhered to Superfrost Plus microscopy slides and used for staining. Sections were stained for general morphology observations with hematoxylin and eosin (H&E).

Immunofluorescent staining with specific antibodies was performed to detect the presence of blood vessels (CD-31), collagen type I and elastin. Frozen sections were fixed with ice cold methanol for 10 min and rinsed 3 times with Phosphate Buffered Saline (PBS). Sections were blocked for 30 min with PBS-0.05%Tween20 (PBST) containing 20% calf serum (PBST-S) at room temperature. Sections were incubated overnight at 4^{0}C with the primary antibodies in PBST-S. The concentration of each of the primary antibodies was as follows: 10 mg/ml of rabbit anti-rat collagen type 1 (Abcam), 10 mg/ml of rabbit anti-rat elastin (Chemicon) and 20 mg/ml of mouse anti-rat CD31 (AbD Serotec, Oxford, UK). One hour room temperature incubation with Cy3-conjugated anti-mouse or anti-rabbit antibody (Jackson ImmunoResearch Lab., West Grove, PA) was used for visualization. Co-staining of sections with fluorescein labeled wheat germ agglutinin (WGA; 5 mg/ml; Molecular Probes, Eugene, OR) was used for general visualization of the sample structure. Nuclei were stained by 5 min incubation with a DAPI solution (Sigma, St. Louis, MO) in PBST. The sections were examined and photographed with a Leica microscope.

3.2.3.1 Morphology of 3D BLB constructs in vitro

Prior to utilization for implantation, histological analysis of the BLB constructs with H&E showed the presence of areas resembling bone at both ends of the constructs **(**Figure 3.2**A)**. The fibrous middle part of the BLB constructs resembled ligament **(**Figure 3.2**A)**. At the higher magnification the type I collagen stained bone portion showed dense deposits of collagen **(**Figure 3.2**B and D)** similar to those found in the developing bone *in vivo*. Type I collagen immunostaining of the ligament portion of the BLB construct revealed well aligned longitudinally oriented collagen fibers, some evidence of crimp morphology and elongated nuclei between fibers **(**Figure 3.2**C and E)**. The middle part of the BLB constructs also stained positive for elastin **(**Figure 3.2**F)**. The ligament portions of the 3D BLB constructs self-assemble *in vitro* around previously formed engineered bone constructs (EBCs). The absence of DEX in the ligament media produces unmineralized ECM that displays evidence of the characteristic crimp morphology of type I collagen fibrils *in vitro*. The ligament region development *in vivo* includes increased type I collagen content, improved collagen organization and more consistent crimp morphology and the development of a continuous, aligned elastin network.

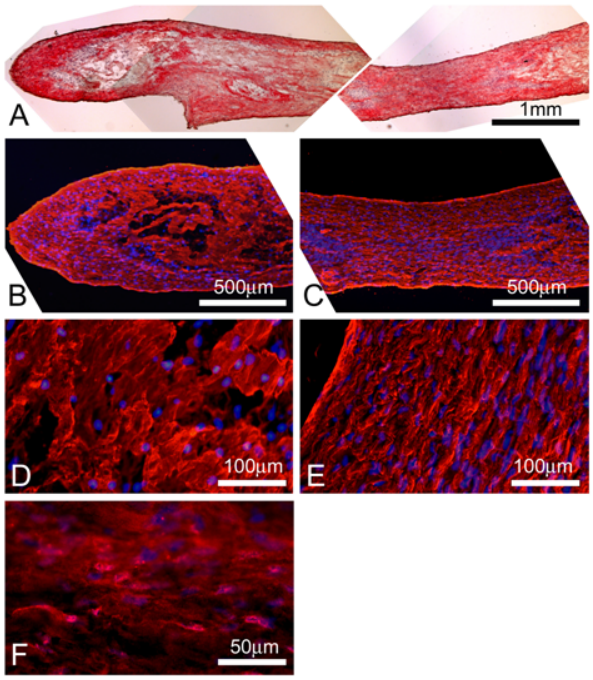

Figure 3.2 Histological evaluation of the 3D BLB construct developed *in vitro*. (A): H&E staining. (B) and (D): collagen 1 immunostaining (red) of the end of the construct. (C) and (E): collagen 1 (red) immunostaining of the middle part of the construct. (F): elastin immunostaining (red) of the middle part of the construct. DAPI staining (blue) was used to visualize the nuclei [53].

3.2.3.2 Morphology of 3D BLB explants

During either one or two months of implantation, the BLB constructs replaced the MCL in the left leg of the host rat model. Both one- and two-month explants were comparable in structure, with 2-month explants showing slightly more advanced structural features. Therefore, only the 2-month explants data are shown. When explanted, the constructs were integrated well into the native bone at both the tibial and femoral sites **(**Figure 3.3**)** and were supplied by the blood vessels generated from the host animal. Longitudinal sections of the middle of BLB explants were stained with H&E **(**Figure 3.4**).** Collagen fibers filled the entire middle part of the explant with more cellular areas located at the periphery **(**Figure 3.4**A-C)**. While the collagen fibers in the explants were highly organized and resembled that of native adult rat MCL **(**Figure 3.4**E)**, the explants displayed a higher nuclei per collagen fiber ratio placing them between neonatal **(**Figure 3.4**D)** and adult **(**Figure 3.4**E)** MCL**.**

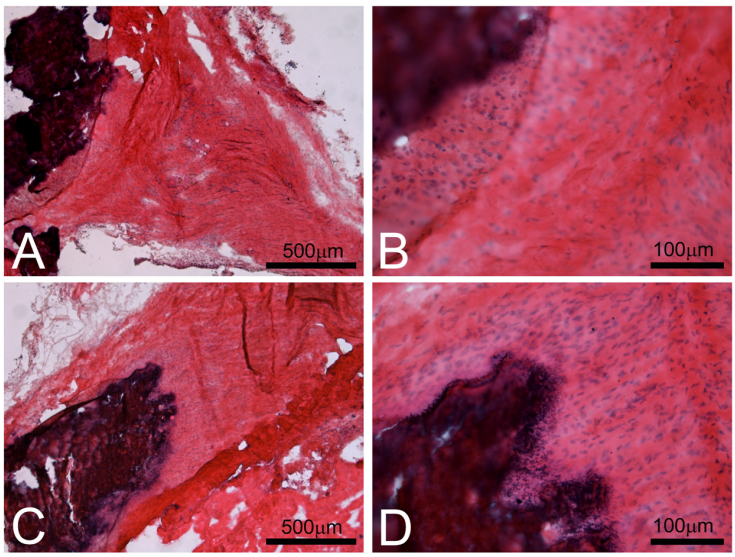

Figure 3.3 H&E staining of areas of native bone/ 3D BLB construct interfaces at the tibia (A-B) and femur (C-D) sides after 2 months of implantation [53].

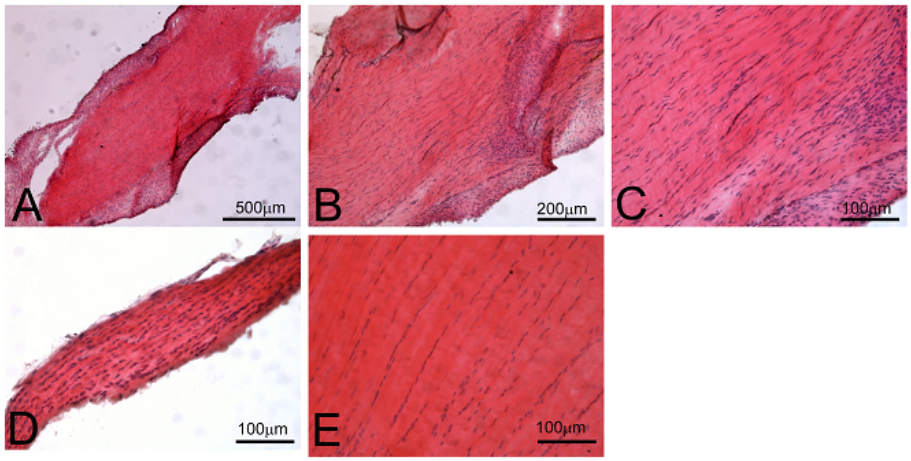

Figure 3.4 H&E staining of the middle part of the 3D BLB construct after 2 months of implantation (A-C) and native MCL ligament from 21 day old neonatal (D) and from adult (E) rat [53].

Immunostaining of the middle of the BLB explants for type I collagen **(**Figure 3.5**A and B)** showed patterns of more densely packed collagen fibers than those found in neonatal MCL **(**Figure 3.5**C)** and more closely resembled type I collagen staining of adult rat MCL **(**Figure 3.5**D).** Blood vessels were easily detected at the periphery of the middle part of the BLB explants **(**Figure 3.6**A and B).** The degree of vascularization was slightly higher than that found in the native neonatal **(**Figure 3.6**C)** and adult **(**Figure 3.6**D)** rat MCL. The elastin immunostaining of the middle of the BLB explants detected very thin

longitudinally oriented elastic fibers **(**Figure 3.7**A).** The elastin content was higher than that found in the 3D BLB constructs *in vitro* but lower than in the native neonatal **(**Figure 3.7**C)** and adult **(**Figure 3.7**E)** rat MCL.

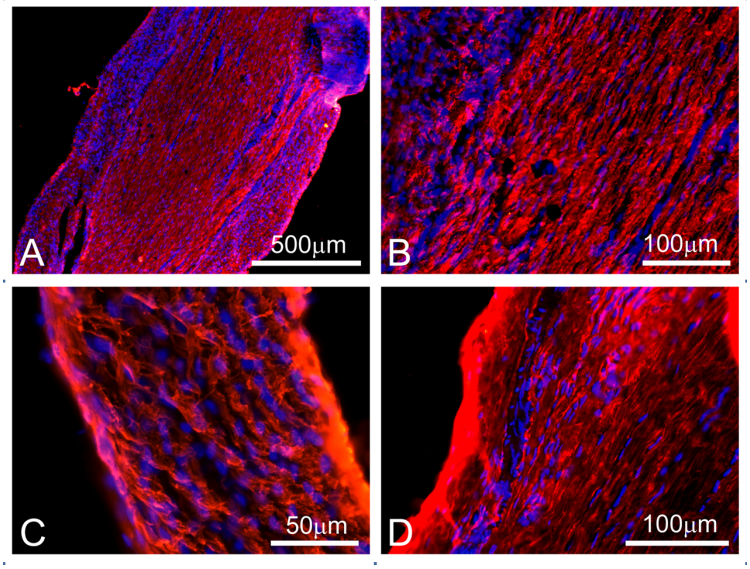

Figure 3.5 Immunostaining of the middle part of 3D BLB construct after 2 months of implantation (A and B) and native MCL ligament from 21 day old neonatal (C) and from adult (D) rat with antibodies against collagen 1 (red). DAPI staining (blue) was used to visualize the nuclei [53].

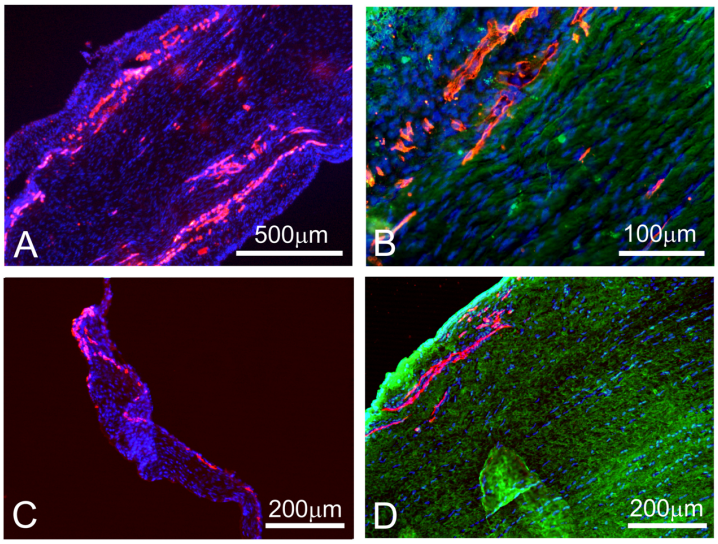

Figure 3.6 Immunostaining of the middle part of 3D BLB construct after 2 months of implantation (A and B) and native MCL ligament from 7 day old neonatal (C) and from adult (D) rat with antibodies against CD31 (red) to visualize blood vessels. DAPI staining (blue) was used to visualize the nuclei. WGA lectin-fluorescein (green) was used to visualize the general tissue structure [53]

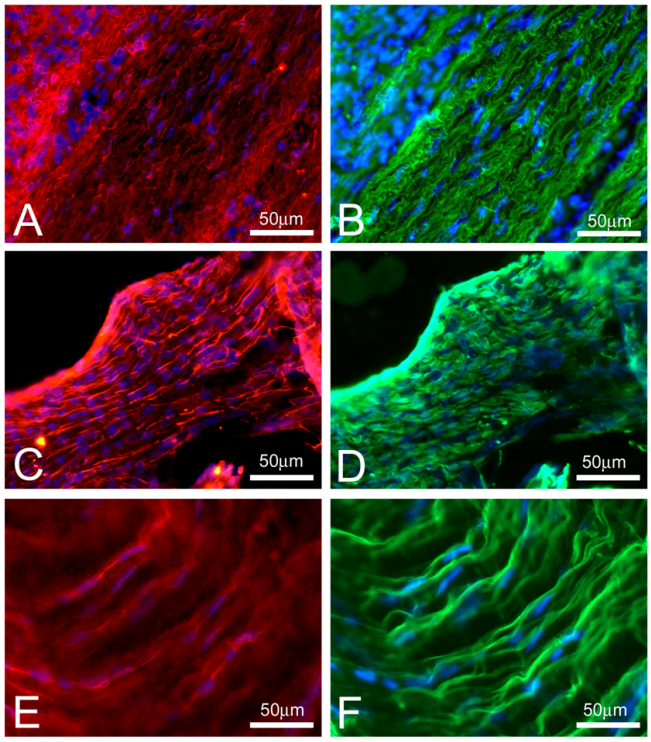

Figure 3.7 Immunostaining of the middle part of 3D BLB construct after 2 months of implantation (A) and native MCL ligament from 7 day old neonatal (C) and adult (E) rat with antibodies against elastin (red). DAPI staining (blue) was used to visualize the nuclei. WGA lectin-fluorescein (green in B, D and F) was used to visualize the general tissue structure in 3D BLB construct (B), 7-day old neonatal (D) and adult (F) rat [53].

3.2.4 Summary of engineered BLBs used as MCL replacements

The present approach avoids the use of a resorbable scaffold and adopts a design rubric based on the concept of displacement or strain controlled rather than load (or stress) controlled mechanical requirements of knee ligaments. The mechanics on the engineered BLBs used rat MCL replacements will be discussed in detailed in **Chapter 4**. After either one or two months *in vivo* as a replacement for the medial collateral ligament (MCL) of a rat, the bone portion of 3D BLB constructs integrated well with the native bone. The ligament region of the rat 3D BLB constructs showed the presence of aligned, crimped, type 1 collagen and elastin. The regenerated extracellular matrix on these engineered BLB explant demonstrated its great potential of use as a ligament graft.

3.3 BLB constructs used as ACL grafts in sheep model

The successful outcome of the engineered BLB used as MCL replacement in rat demonstrated the efficacy of this scaffold-less co-cultured technique and also suggested its great potential as an ACL graft. For ACL replacement studies, a rat model is not ideal because its knee joint is small. The sheep and goat have commonly been chosen as large animal models for the knee [55-58] because of anatomical [59-62] and mechanical [63-66] similarities to human ACLs. We therefore scaled the geometry of the tissue engineered BLB up to match the size of a sheep ACL, then studied its use as an ACL replacement in the sheep model. We first characterized the morphological and mechanical properties of BLB explants after 2, 3, 4 and 6 months (Study 1). The purpose of this study was to engineer a 3D multi-phasic ligament model or BLB construct that will rapidly grow and remodel in vivo to attain biomechanical properties of native ACL. Preliminary results showed well organized extracellular matrix in BLB explants after 6 months in vivo. We then conducted a 9-month in vivo study using the BLB as an ACL graft with a patellar tendon autograft, as a surgical control (Study 2). The purpose of Study 2 was to compare the tissue engineered construct to a commonly used graft, the patellar tendon, physically, functionally and morphologically. To understand which cells determine the development of the engineered construct site, we used male bone marrow stromal cells to track (PCR) cell migration in female sheep.

3.3.1 *In vitro* co-culture of the bone-ligament-bone (BLB) construct

3.3.1.1 Preparation of solutions and media

The solutions and media used to create sheep BLB constructs are the same as the ones used for rat BLB constructs. Please refer to section **3.2.1.1** for a detailed description.

3.3.1.2 Preparation of culture dishes

Cell culture plates (100 mm in diameter) were used to culture ligament cells and 35mm cell culture plates were used to culture bone cells. A portion of 100 mm cell culture plates was coated with 12.0 ml of Sylgard for use of securing

3D constructs. These sylgard coated dishes were allowed to cure for 3 weeks prior to use. Plates were then filled with 20 ml of DPBS, decontaminated with UV light (wavelength 253.7 nm) for 90 minutes, and placed in a 37°C 5% CO_2 incubator for 1 week prior to use.

3.3.1.3 Sheep BMSCs isolation and expansion

BMSCs were collected from adult female black suffolk sheep and male lambs for different study purposes. Adult sheep were euthanized using 15mL of Fatal Plus (Vortech Pharmaceuticals, Dearborn, MI) and lambs, 4mL. The marrow from a single femur was scooped using a spatula into a 50 ml conical filled with DMEM and 2% antibiotic antimycotic solution. BLBs used for Study 1 (2,3,4 and 6 months implantation) were made from adult female sheep. BLBs used for Study 2 (9 months implantation) were made from male lambs. Briefly, the marrow was minced with scissors, vortexed and pelleted using centrifugation (AccuSpin FR; Beckman Coulter Inc., Fullerton, CA) at 2500 rpm for 10 minutes at 25ºC. The supernatant was aspirated and the cell pellet was resuspended and divided equally into three 100 mm diameter tissue culture dishes for ligament differentiation and one 100 mm diameter dish for bone differentiation. Each dish was fed with 8 ml GM. The bone dish was supplemented with DEX additionally (this held true for the rest of the BLB fabrication). The dishes were incubated at 37ºC, 95% humidity, and 5% CO_2. After 48 h, the non-adherent cells were removed by aspriating the old media and flushing the plates with DPBS three times. Then, all plates were fed with fresh GM. The adherent BMSC were cultured to 80% confluence, at which time cells were enzymatically removed from the 100 mm plate using a 0.25% trypsin-EDTA solution (Gibco) and passaged at a one to three ratio. Cells used to fabricate BLBs were from the third through fifth passages.

3.3.1.4 Sheep BLB construct formation in vitro

Self-organized bone constructs were engineered as previously described [Syed-Picard 2009]. Refer to **3.2.1.4** for a detailed fabrication description. Briefly, as shown in Figure 3.8, BMSCs were first isolated from sheep femurs (Step [1]).

Cells were proliferated and differentiated into osteoblast-like cells and fibroblast-like cells using growth media and growth factors (Step [2]). The monolayers were carefully transferred from culture dishes to Sylgard coated dishes using sterilized tweezers. 2 x 10^5 bone cells were seeded in 1.5 mL GM onto 35 mm cell culture plates. DM was substituted for GM to induce construct formation. After approximately 2 days, a bone monolayer was formed on each dish. (Step [3]). Ligament monolayers were made in a similar fashion: 8 ml of the cell suspension containing 1.3 x 10^6 ligament cells was plated in each 100 mm culture dish. The dishes were placed in a 37ºC 5% CO_2 incubator and the medium (GM) was changed every 2–3 days. After the cells became confluent, approximately three days later, a ligament monolayer had formed on each 100 mm culture dish. (Step [4]). The bone monolayers were transferred from the current culture dishes to Sylgard coated dishes with two minutien pins placed on the monolayers approximately 20 mm apart to guide the formation of 3-D bone constructs (Step [5]). The ligament monolayers were carefully transferred to Sylgard coated 100 mm dishes. Two of the engineered bones previously described were pinned on top of a ligament monolayer, and in-line axially so that the inner ends were 30-40 mm apart, to fabricate a 60-80 mm long BLB (Step [6]). At this point DM replaced GM for ligament. The individual BLB constructs had a diameter of 0.6 to 0.8 mm. Within one week of implantation eight of these constructs were pinned together laterally at their bone ends. Constructs fused together laterally to form a larger width construct with dimensions of approximately 60 to 80 mm long, 2.8 to 3.2 mm in diameter (Step [7]). The BLB constructs did not develop a necrotic core during this period of time *in vitro*. The BLB constructs were then used for implantation as a sheep ACL replacement (Step [8]).

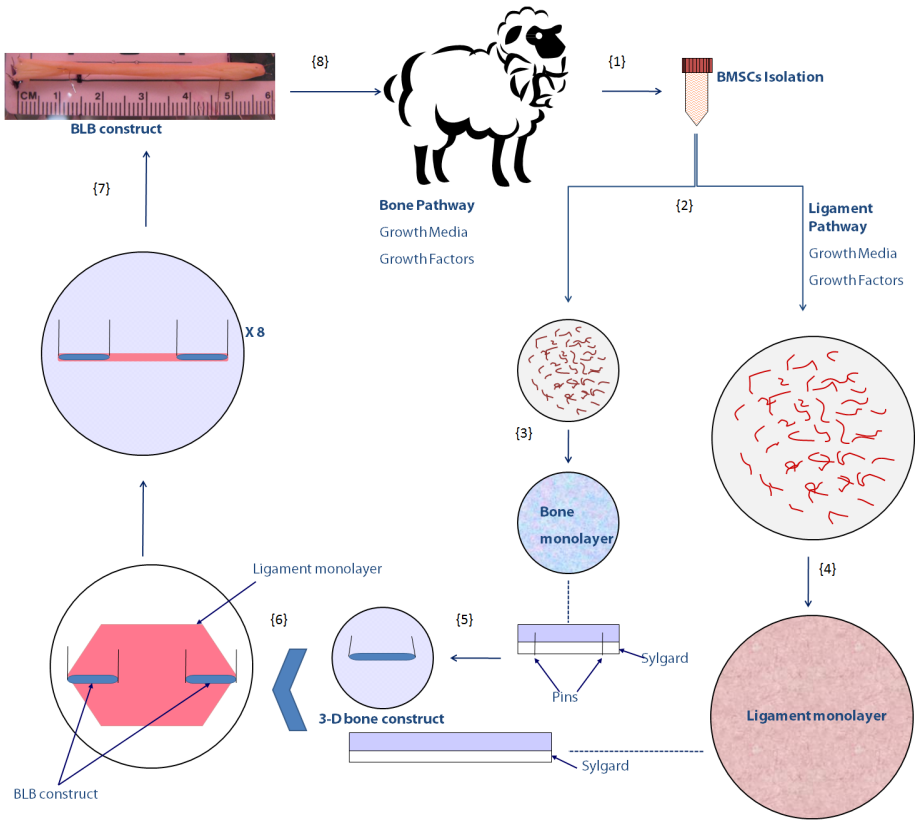

Figure 3.8 Fabrication process of a BLB construct in vitro. BMSCs were first isolated from sheep femurs (Step [1]). Cells were proliferated and differentiated into bone-like cells and ligament-like cells using growth media and growth factors (details can be found in the Methods Section (Step [2]). Bone cells were seeded onto 35 mm cell culture plates. Cells became confluent and a bone monolayer was formed on each dish (Step [3]). Ligament cells were seeded onto 100mm cell culture plates. In the same fashion, cells became confluent and a large ligament monolayer was formed on each dish (Step [4]). The bone monolayers were transferred from the current culture dishes to Sylgard coated dishes with two minutien pins placed on the monolayers approximately 20 mm apart to guide the formation of 3-D bone constructs (Step [5]). The ligament monolayers were carefully transferred to Sylgard coated 100mm dishes. Two of the engineered bones previously described were pinned on top of a ligament monolayer, and in-line axially so that the inner ends were 30-40 mm apart, to fabricate a 60-80 mm long BLB (Step [6]). Within one week of implantation eight of these constructs were pinned together laterally at their bone ends. Constructs fused together laterally to form a larger width construct with dimensions of approximately 60 to 80 mm long, 2.8 to 3.2 mm in diameter (Step [7]). The BLB constructs did not develop a necrotic core during this period of time in vitro. The BLB constructs were then used for implantation as a sheep ACL replacement (Step [8]) [67].

3.3.2 *In vivo* sheep BLB construct used as ACL replacement

3.3.2.1 Animal model and animal care

Black Suffolk female sheep were used as hosts and BMSC donors for the fabricated BLB constructs. These sheep were obtained from the Michigan Livestock Exchange, various farms in the area or intra−university transfer. All

animals were acclimated to our Sheep Research Facility at the University of Michigan for one week prior to any procedure. Sheep were allowed to free range in the pasture until used for surgical implantation. The animals were given access to food and water ad libitum. Femur and tibia bones were surgically dissected under aseptic conditions from the sheep immediately following euthanasia with Fatal Plus (Vortech Pharmaceuticals), to obtain bone marrow for BLB construct fabrication. The BLB constructs were implanted into the ACL site as a replacement tissue and the animals were allowed to recover for either two, three, four or six months before explantation. All surgical procedures were performed in an aseptic environment with anesthesia induced by i.v. injections of Ketamine and Diazepam and sustained with inhalation of halothane gas. After any surgical procedure, the animals were singly housed in secluded pens for two weeks and then released back into the herd until the date of explantation. All animal care and animal surgeries were in accordance with The Guide for Care and Use of Laboratory Animals (Public Health Service, 1996, NIH Publication No. 85-23); the experimental protocol was approved by the University Committee for the Use and Care of Animals.

3.3.2.2 Sheep ACL replacement surgical techniques and procedure

In study 1, ACL replacements were performed open. In study 2, ACL replacements were performed arthroscopically. 20 mls of Marcaine 1% with 1:200,000 epinephrine had been injected in the knee for hemostasis. Two 6 mm incisions were made at the joint line on either side of the patellar tendon. The anterior cruciate ligament was identified and excised leaving a remnant of the ACL stump on both the femur and tibia to aid in positioning the ACL graft (Figure 3.9 **C**-**G**). Drill guides were used to position guide pins in the center of the tibial and femoral footprints. Cannulated reamers were used over the guidewires to fashion 5-6 mm bone tunnels. The graft was passed through the bone tunnels with a suture attached to the proximal end of the graft. Minimal tension (<2 lbs) was applied to the graft as the proximal and distal ends were sutured to the periosteum with the knee in 30 degrees of flexion.

For Study 2, a 5mm diameter patellar tendon autograft (PTG) (Figure 3.9**B**) was used in a similar fashion using 7 mm femoral and tibial tunnels. 10 mm long bone plugs from patella and tibia were fashioned with an oscillating saw. A suture was attached to each end of the PTG for fixation. Approximately 5 lbs of tension was applied to the PTG as the proximal and distal ends were sutured to the periosteum with the knee in 30 degrees of flexion (Figure 3.9**H**).

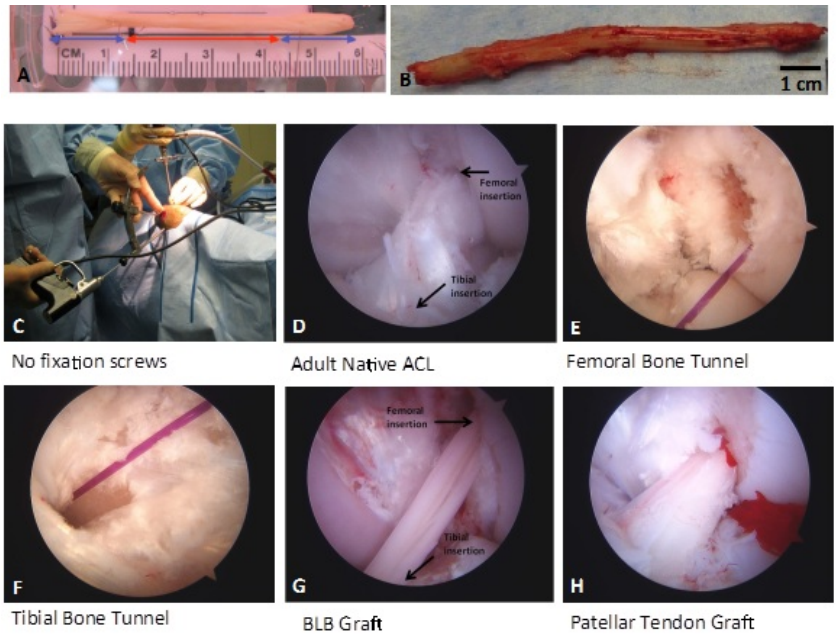

Figure 3.9 Arthroscopic ACL replacement in sheep utilizing BLB constructs and PT autografts. In vitro BLB construct prior to the surgery (A) has a total length of 70 mm including a 30 mm long ligament portion and two 20 mm long bone ends. A freshly harvested PTG (B) is about 11 cm long and 4-5 mm wide prior to the surgery. Both surgeries were done arthroscopically without utilizing interference screws for fixation (C). The landmarks of the ACL insertions on femur and tibia were located (D). Then the ACL was removed and the tunnels (E, F) were drilled through the insertion landmarks. The BLB construct (G) or PTG (I) was guided through the tibia and femur tunnels using the suture attached to the proximal ends of the grafts.

During recovery, the animals were placed on a heat pad and covered with a blanket to maintain body temperature; respiration rate and other vital signs were monitored until the animal was standing. Once standing, the animal was moved to a pen and given access to food and water. Daily monitoring of the surgical site for infection was conducted. The sutures were removed at 14 days post surgery.

3.3.2.3 BLB explant, native ACLs, and patellar tendon dissections

After two, three, four, six and nine months of implantation, BLBs, contralateral native ACLs, native patellar tendons and PT autografts (9-month) were dissected for morphological and mechanical analyses. Sheep were euthanized with Fatal Plus. The knees were dissected, removing the skin and muscle but maintaining the ligament connections at the knee. The patellar tendon with patella was first released from the patellofemoral groove and dissected to expose its tibial insertion. The patellar tendon with insertions intact was then removed from the knee and preserved for uniaxial tension tests. Then, the surrounding tissue was dissected, keeping the majority of the knee capsule intact. The tibia and femur were cut at mid-substance to provide substantial area to grip the specimen during mechanical testing. The knee specimen first underwent 45 degrees anterior drawer tests. The ACL, PT autograft and BLB were then isolated by removing all other knee ligaments and menisci. To visualize the deformation of the ACLs, PT autografts and BLBs, the medial condyle was carefully removed to reveal the entire tissue with insertion.

3.3.3 Growth of BLB constructs and PT autografts during ACL replacement

In Study 1, the dimensions of the ligament portion of the in vitro BLB constructs prior to implantation (N=7) were approximately 30-40 mm in intra-articular length and 3.0±0.2 mm in diameter (7.1±1.0 mm^2 in cross sectional area (CSA)). The BLB constructs we have designed are viscoelastic and they contain contractile cells. Prior to implantation they are longitudinally constrained and carry an internal tensile stress. At the time of insertion into the bone tunnel, they undergo viscoelastic deformation to restore this passive tension. The initial compliance of the intra-articular region of the BLB graft and its ability to maintain self-tension allow it to accommodate knee motion and not slip or develop slack. The sizes and structures of adult native ACL were compared to that of our BLB explants at the time of dissection at two-, three-, four- and six-month recovery time points (Figure 3.10**A**-**E**). The native ligaments (Figure 3.10**F**) were taken

from the contralateral knees of animals at the six-month recovery period time point. These results demonstrate that the BLB constructs rapidly grew physically in cross section during the initial implantation period and reached the size of native adult ACL at about four months after implantation.

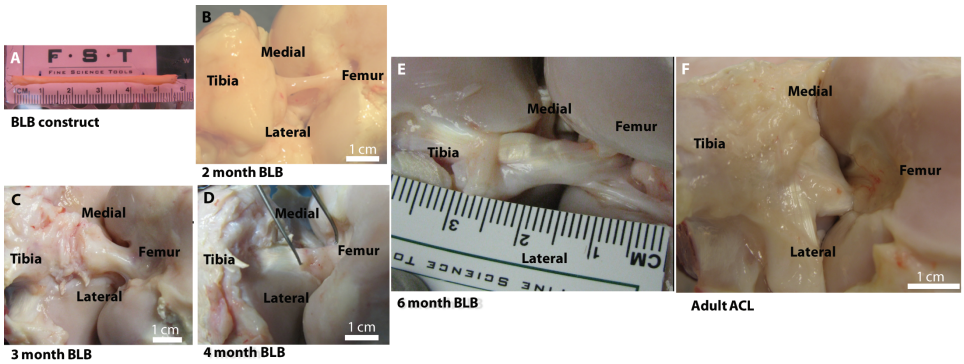

Figure 3.10 BLB construct *in vitro* (A) 30-40 mm in intra-articular length by 7.1±1.0 mm^2 CSA, [N=7]; BLB explant *in vivo* at (B) two: 17 mm long by 14 mm^2 CSA [N=1], (C) three: 18 mm long by 28 mm^2 CSA [N=1] (D) four: 18 mm by 64 mm^2 CSA [N=1] and (E) six months: 16.3±1.1 mm long by 57.5±48.7 mm^2 CSA [N=4]; native adult ACL: 18.5±0.8 mm long by 27.7±4.3 mm^2 CSA [N=3] (F) [67].

In Study 2, BLB constructs prior to implantation (N=7) were 30-40 mm in length, 3.0±0.2 mm in diameter, and 7.1±1.0 mm^2 in cross sectional area (CSA). After 9 months in vivo recovery, the CSA of BLB explant (37.0±5.5 mm^2) grew to the size of the contralateral ACL (N=14, 35.4±1.7 mm^2). No significant differences were found between the BLB and the ACL CSA (*p=0.81*). The CSA of the PTG prior to implantation was 18.9±1.0 mm^2. After 9 months of recovery, the CSA of PTG CSA (N=7, 57.6±6.7 mm^2) was significantly larger than that of the contralateral ACL (*p<0.025*).

3.3.4 Morphological characterization of the sheep BLB in vitro, BLB explant, PT autograft, native ACL and PT

Similarly to section **3.2.3**, histochemical and immunofluorescent staining was conducted to obtain the cell viability, the morphology of extracellular matrix, vascularization, and innervation of the sheep BLBs in vitro, BLB explants, PT autografts, native ACLs and native PTs. Unless otherwise indicated, all sample

preparation and analysis were conducted following the same protocols developed previously and detailed can be found in section **3.2.3**.

In addition to detecting the type I collagen, elastin, blood vessels (CD-31) and innervation (NCAM), immunofluorescent staining with specific antibodies for lubricin was also performed on these samples to detect the presence of lubricin. The concentration of each of the primary antibodies was as follows: 10 µg/ml of rabbit anti-NCAM, rabbit anti-collagen type 1 and rabbit anti-elastin (all from Millipore); 10 µg/ml of rabbit anti-lubricin (Abcam,); and 10 µg/ml of rabbit anti-CD31 (Abbiotec).

3.3.4.1 Analysis of structure of in vitro sheep BLB prior to implantation

Our previous studies have shown that the bone ends of the BLBs in vitro stain for mineralization activity (Alizarin Red). We have also shown the absence of markers for bone (Alizarin Red) and cartilage (type II collagen) in the mid-section of the BLB constructs. The mid-sections stained for type I collagen indicating fibrogenic differentiation. Newly formed bone had areas of collagen-rich matrix with cells trapped inside the matrix (arrow in Figure 3.11**A** and **B**). The mid-sections stained for type I collagen showed longitudinally oriented collagen fibers indicating fibrogenic differentiation (Figure 3.11**C**).

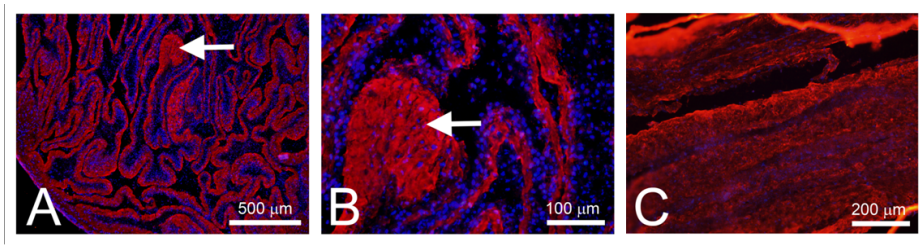

Figure 3.11 Section of bone (A and B) and ligament (C) portions of BLB construct before implantation stained with antibody against collagen type 1 (red in A-C) and nuclear stain DAPI (blue in A-C). Arrows show area of the newly formed bone with cells trapped in the collagen-rich matrix.

3.3.4.2 Analysis of structure, vascularization, and innervation of the BLB explant after 2, 3, 4 and 6 months in vivo recovery

After 6 months of implantation in vivo, we compared cross sections at the centers of all BLB explants with those of the native ACL. Figure 3.12 shows H&E staining of cross sections through the centers of our BLB explants after 6 months in vivo (N=4). Figure 3.12**A** and 4**B** show the cross sections of the BLB explants fabricated using frozen BMSCs whereas Figure 3.12**C** and **D** show the cross sections of the BLB explants fabricated using fresh BMSCs. In constructs made from frozen cells (Figure 3.12**A** and **B**), the center of the section contained viable cells and was also highly vascularized (arrow in Figure 3.12**A** and **B**) suggesting the BLB was fully viable and actively remodeling and growing but that more time was needed in vivo to fully fill out the section with ligament tissue. In constructs made from fresh cells (Figure 3.12**C**), we see evidence of the initial fascicle formation. In Figure 3.12**D** (arrows) we see a fully remodeled BLB with collagen fascicle size and structure that very closely resembles that seen in adult native ACL (arrows in Figure 3.12**E**).

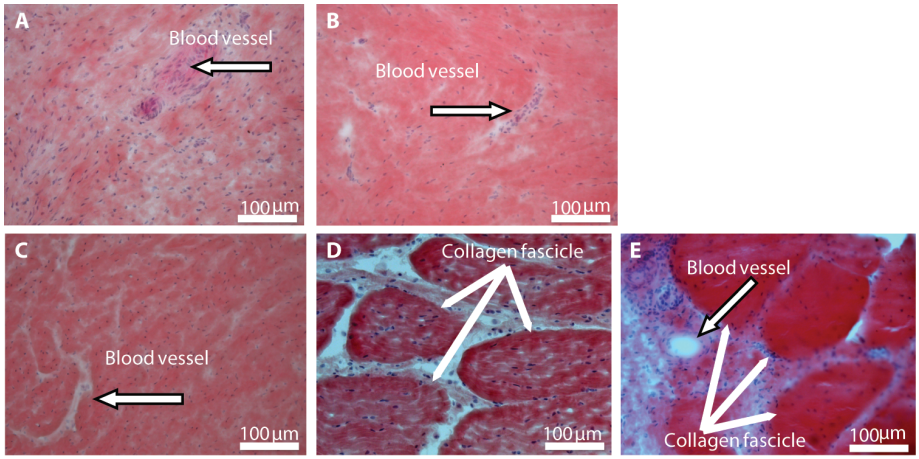

Figure 3.12 H&E staining of cross-sections of BLB explants after six months of implantation in vivo as an ACL replacement (A, B, C and D) and of native adult ACL (E). The center of section (A and B) made from frozen BMSCs contained viable cells and was highly vascularized but did not have well formed collagen fascicles. The cross section (C) made from fresh cells suggests possible collagen fascicle formation. Explant (D) made from fresh cells also appeared to have fully remodeled with collagen fascicle size and structure that very closely resembled that seen in adult native ACL in (E).

We analyzed frozen sections of the middle portion of the BLB explants for the presence of both blood vessels and nerves, using anti-CD31 and anti-NCAM antibody immunostaining, respectively (Figure 3.13). CD31 (PECAM1) is a member of the immunoglobulin superfamily. It is a major constituent of the endothelial cell intercellular junctions and is considered to be a specific marker for blood vessels. NCAM (neural cell adhesion molecule) is expressed in all neurons from very early in the development. It is considered to be a specific marker for the neuronal cell bodies, axons and dendrites. We found, after following a three-month recovery, the midsection of the BLB-replaced ACL contained an extensive vasculature (Figure 3.13**B**). The vasculature was greater than that observed in adult tissues and equivalent to that of a 14-day-old native neonatal sheep ACL (Figure 3.14**E**). Additionally, we observed innervation of nerve in the midsection of the replaced ACL (Figure 3.13**C**, **F**, and **I**). After a four-month recovery, the midsection of the replaced ACL had larger and more organized blood vessels and nerves (Figure 3.13**E** and **F**) and continued further organization of blood vessels and nerves was seen following a six-month recovery (Figure 3.13**H** and **I**). H&E staining of these same explants showed more organized collagen fibers with time in vivo (Figure 3.13**A**, **D**, and **G**).

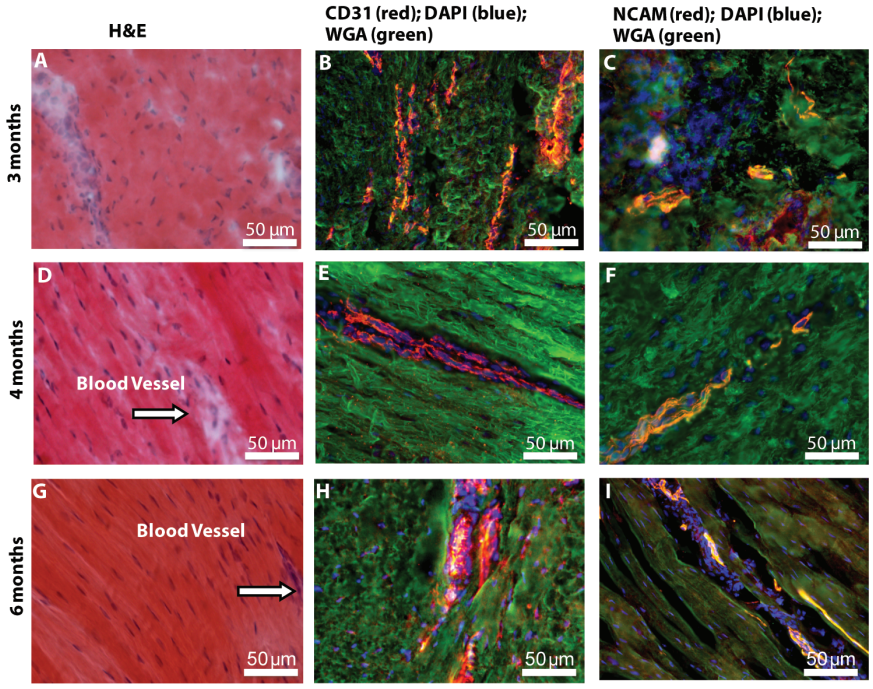

Figure 3.13 Longitudinal sections of BLB explants after (A-C) three, (D-F) four, and (G-I) six months of implantation *in vivo* as an ACL replacement. (A, D & G) H&E staining for visualization of general structure and collagen fibers; (B, E & H) CD31 immunostaining for visualization of blood vessels; (C, F & I) NCAM immunostaining for visualization of nerves.

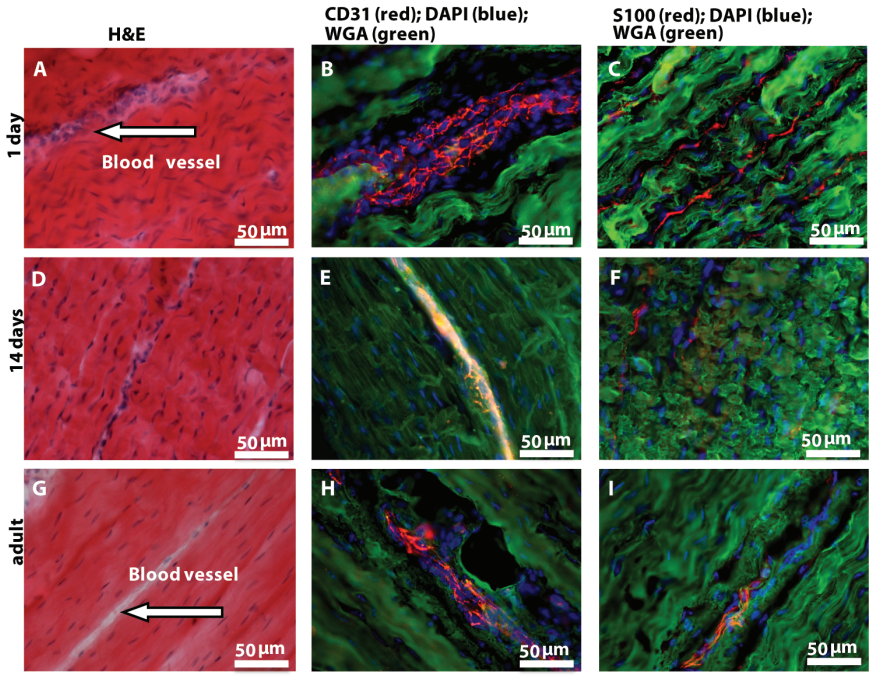

Figure 3.14 Longitudinal sections of neonatal and adult native sheep ACL. Pictures of (A-C) one day old, (D-F) 14 day old and (G-I) adult sheep ACL are shown. (A, D & G) H&E staining for visualization of general structure and collagen fibers; (B, E & H) CD31 immunostaining for visualization of blood vessels; (C, F & I) S-100 immunostaining for visualization of nerves.

These data suggest that our tissue engineered BLBs remodeled in vivo with respect to mechanical structure (collagen alignment) and biological function as indicated by the vascularization and innervation. To compare the explants with native sheep ligaments, we stained frozen longitudinal tissue sections from one-day, 14-day and adult sheep ACL for general structure, vascularization and innervation (Figure 3.14). The innervation and vascularization of the BLB explants at six months (Figure 3.13**H** and **I**) in vivo resembles that of the adult ACL (Figure 3.14**H** and **I**).

3.3.4.3 Analysis of BLB/native bone interface

Figure 3.15 shows a demineralized longitudinal section of a BLB explant after two months in vivo as an ACL replacement. Within two months as an ACL replacement in the sheep, our BLB constructs integrated well with native tissue to form a structurally viable and biochemically relevant enthesis. Sharpey's fibers (white arrow in Figure 3.15**A**) indicate integration of native bone with the engineered tissue. Aligned nuclei (white arrow) indicative of a fibrocartilagenous region are seen in Figure 3.15**B**.

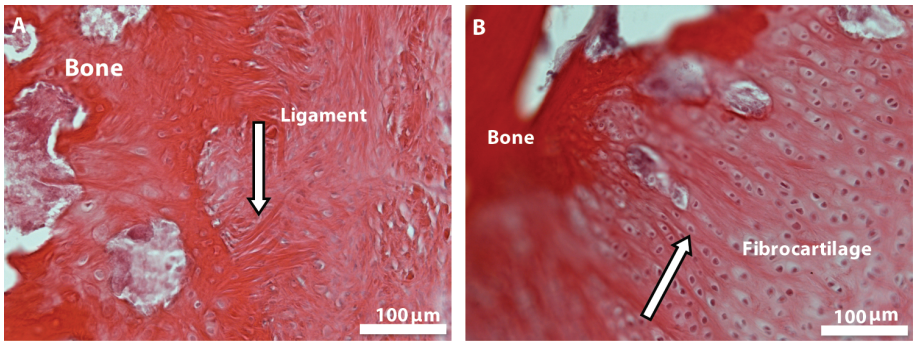

Figure 3.15 BLB explant / native bone interface two months after implantation *in vivo* as an ACL replacement. Two sections of the BLB explant shows (A) integration into native bone through the Sharpey's fibers (arrow) and (B) fibrocartilaginous region with aligned nuclei (arrow).

3.3.4.4 Analysis of structure, vascularization, innervation and elastin of the native ACL, the BLB and the PTG at 9-month

The H&E stained cross sections through the center of the BLB explant after 9 months in vivo showed viable cells (Figure 3.16). Some BLBs (N=2;

Figure 3.16**A**) had remodeled areas with collagen fascicle size and structure that very closely resembled that seen in adult native ACLs (Figure 3.16**B**).

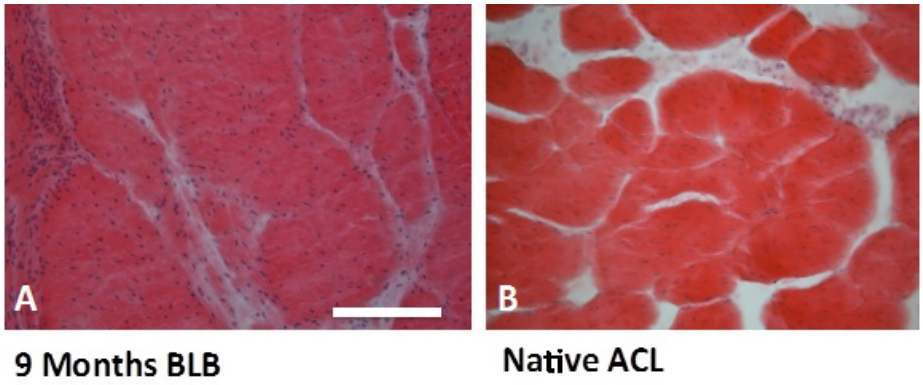

Figure 3.16 H&E staining of cross-sections of BLB explants after 9 months *in vivo* as an ACL replacement (A) and of native adult ACL (B). The center of section (A) appeared to have fully remodeled with collagen fascicle size and structure that very closely resembled that seen in adult native ACL in (B).

Two additional BLBs that were analyzed did not have well developed collagen fascicles. The BLBs were also highly vascularized suggesting that they were fully viable and actively remodeling and growing (Figure 3.17**E**). The overall structure of the extracellular matrix (WGA, collagen type I and elastin staining), vascularization (CD31) and innervation (NCAM) of the BLB explants (N=4; Figure 3.17**D**-**F**) resembled those of the native ACLs (Figure 3.17 **A**-**C**). Collagen in PTGs was less organized than in the ACLs and BLBs (Figure 3.17**G**). More oval shaped tenocytes were found in these PTGs (Figure 3.17**G**) as well as in native PT (not shown) whereas the cells in ACLs (Figure 3.17**A**) or BLBs (Figure 3.17**D**) tended to be more elongated. Some of the PTGs also showed evidence of vascularization and innervation (N=2; Figure 3.17**H**, **I**). However, vascularization and innervation were poor in some PTGs (N=2). Elastin was found in PTGs (Figure 3.18**B**) but to a far lesser extent than in BLBs (Figure 3.18**A**).

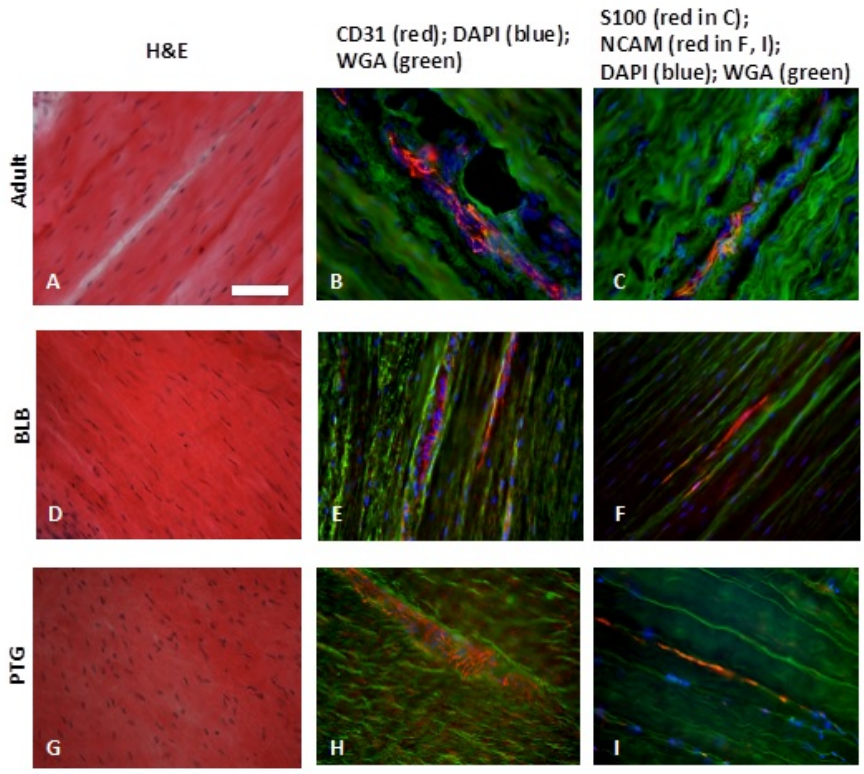

Figure 3.17 Longitudinal sections of native ACL (A-C), BLB explants (D-F) and PTG (G-I) after 9 months *in vivo* as an ACL replacement. (A, D & G) H&E staining for visualization of general structure and collagen fibers; (B, E & H) CD31 immunostaining for visualization of blood vessels; (C, F & I) NCAM immunostaining for visualization of nerves. All images have the same scale bar. Scale bar = 0.05mm.

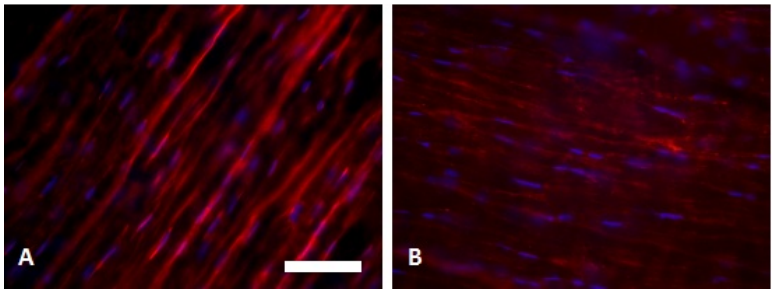

Figure 3.18 Longitudinal sections of BLB (A) and PTG (B) after 9 months in vivo as an ACL replacement immunostaining for elastin. All images have the same scale bar. Scale bar = 0.05mm.

3.3.4.5 Analysis of Lubricin of the ACL, the BLB Explant and the PTG

The cross sections through the center of the ACL not only showed intense lubricin immunostaining along the surface of the ACL but the cells inside the ACL were found to express lubricin (Figure 3.19**A**). The cross sections of BLBs also showed lubricin inside the BLBs (Figure 3.19**B**). PTGs showed very weak

staining for lubricin in the center (Figure 3.19**C**). The BLB cross (Figure 3.19**B**) and longitudinal sections demonstrated lubricin staining (Figure 3.19**E**) resembling that of native ACLs (Figure 3.19**A** and **D**).

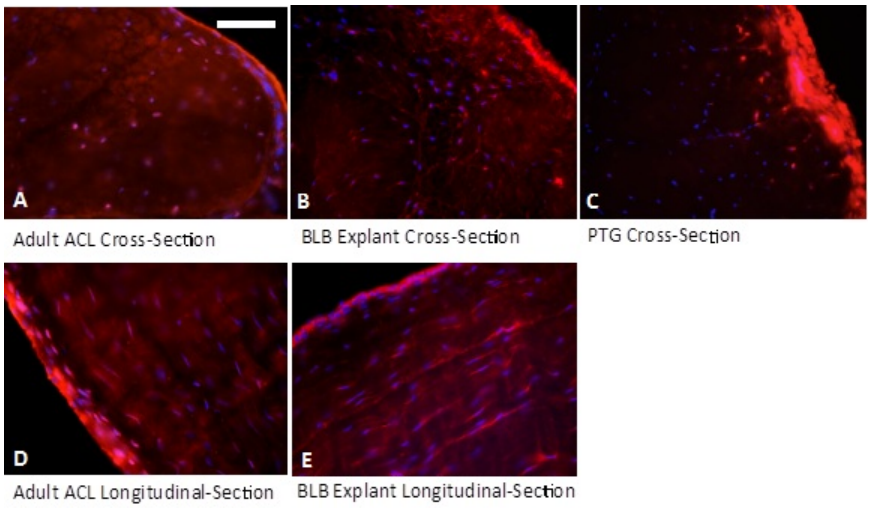

Figure 3.19 Cross-sectional sections of ACL (A), BLB (B) and PTG (C) after 9 months in vivo, and longitudinal sections of ACL (D) and BLB (B) immunostaining for lubricin. All images have the same scale bar. Scale bar = 0.05mm

3.3.5 Y chromosome PCR analysis for BLB explant

Genomic DNA was isolated from tissue samples by proteinase K digestion followed by ethanol precipitation. A PCR based assay for the ovine-specific Y-chromosome repeat sequence *Ucd043* was used to determine the presence of male cells in BLB explant samples [68]. Duplex PCR was performed using SCUcd043.FWD/SCUcd043. REV primers to amplify *Ucd043* together with P1-5EZ/P2-3EZ primers to amplify the ZFY/ZFX locus. P1-5EZ and P2-3EZ primers also provided an internal control for amplification. Sensitivity of the assay was assessed with a dilution panel of 100, 25 and 5 pg of male ovine DNA. Subsequent experimental reactions were carried out with 25 ng of genomic DNA template.

In the PCR assay sensitivity tests, dilutions containing as little as 5 pg of male DNA were reliably detected (Figure 3.20**A**). However, we were unable to detect the presence of Y-chromosome from tibial, middle or femoral regions of

BLB explants using up to 25 ng of genomic DNA template (N=4; Figure 3.20**B**). The ZFY/ZFX internal PCR control amplified efficiently for all samples and large amounts of female DNA were present.

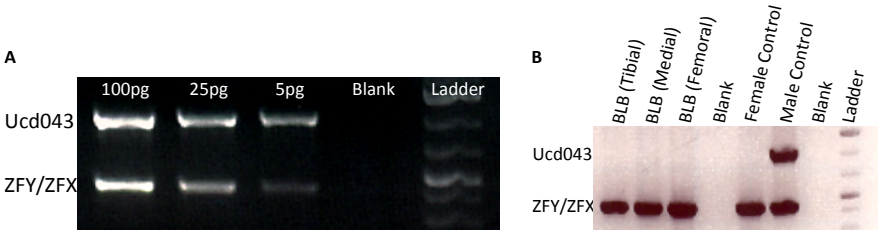

Figure 3.20 Y-Chromosome PCR assay sensitivity test (A) showed the Y-chromosome locus *Ucd043* (upper band) was reliably detected from dilutions of 100, 25 and 5 pg of male ovine DNA. The lower band corresponds to the ZFY/ZFX locus present on both X- and Y-chromosomes and acts as an internal PCR control. Y-Chromosome is undetectable in BLB Explants by PCR Analysis (B). Lanes 1-3, genomic DNA from BLB explants; lane 4, no template; lane 5, genomic DNA from female sheep; lane 6, genomic DNA from male sheep; lane 7, no template; lane 8, 1 Kb Plus DNA Ladder (Invitrogen). Reactions contained 25 ng of template DNA. Upper band corresponds to *Ucd043* PCR product which is specific to the Y-Chromosome and lower band corresponds to the ZFY/ZFX positive control.

3.3.6 Summary

The resulting 3D multi-phasic bone-ligament-bone (BLB) constructs exhibit the structural and functional interface characteristics of native rat MCL and sheep ACL by utilizing engineered ligament with engineered bone at each end. We hypothesize that the BLB constructs can integrate into the recipient bone to form a mechanically viable and biochemically relevant interface between the two tissues and allow rapid growth of the BLB construct to attain histological properties that resemble those of native, adult ACL [67]. The ingrowth of blood vessel and nerve demonstrates the incorporation of our tissue engineered BLB graft in the host. The complete replacement of the cell population in our 9-month comparison study (**3.3.5**) further demonstrates its successful integration and is consistent with previous goat ACL research [69]. The superficial and deep presence of lubricin in the BLB is exciting, knowing the importance that this protein plays in normal joint function [70, 71]. The elastin pattern of the BLB is similar to that of the contra-lateral ACL (data not shown); more so than that of the PTG. Elastin is not seen in the BLB in vitro and represents “ligamentization” of the engineered construct.

3.4 Conclusions

In our rat MCL replacement study, we demonstrate that the engineered BLB construct has great potential for use as a ligament due to its ability to generate the extracellular matrix that resembles that of he native rat MCL after either one or two months *in vivo* recovery. In the sheep ACL replacement studies, we demonstrate that the engineered BLB has tremendous potential as an ACL replacement as well as an MCL replacement, despite the inhospitable environment of the intra-articular region. The success of our BLB graft as an ACL replacement in our large animal model suggests this approach may have clinical relevance in ACL replacement in humans.

3.5 References

1. Laurencin, C.T. and J.W. Freeman, *Ligament tissue engineering: an evolutionary materials science approach.* Biomaterials, 2005. **26**(36): p. 7530-7536.

2. Yates, E.W., et al., *Ligament tissue engineering and its potential role in anterior cruciate ligament reconstruction.* Stem cells international, 2012. **2012**(Journal Article): p. 438125.

3. Petrigliano, F.A., D.R. McAllister, and B.M. Wu, *Tissue engineering for anterior cruciate ligament reconstruction: a review of current strategies.* Arthroscopy : The Journal of Arthroscopic & Related Surgery : Official Publication of the Arthroscopy Association of North America and the International Arthroscopy Association, 2006. **22**(4): p. 441-451.

4. Ge, Z., et al., *Biomaterials and scaffolds for ligament tissue engineering.* Journal of biomedical materials research.Part A, 2006. **77**(3): p. 639-652.

5. Bernardino, S., *ACL prosthesis: any promise for the future?* Knee surgery, sports traumatology, arthroscopy : official journal of the ESSKA, 2010. **18**(6): p. 797-804.

6. Kuo, C.K., J.E. Marturano, and R.S. Tuan, *Novel strategies in tendon and ligament tissue engineering: Advanced biomaterials and regeneration motifs.* Sports medicine, arthroscopy, rehabilitation, therapy & technology : SMARTT, 2010. **2**: p. 20.

7. Goh, J.C., et al., *Tissue-engineering approach to the repair and regeneration of tendons and ligaments.* Tissue engineering, 2003. **9 (**Suppl 1): p. S31-44.

8. Freeman, J.W., M.D. Woods, and C.T. Laurencin, *Tissue engineering of the anterior cruciate ligament using a braid-twist scaffold design.* Journal of Biomechanics, 2007. **40**(9): p. 2029-2036.

9. Cavallaro, J.F., P.D. Kemp, and K.H. Kraus, *Collagen fabrics as biomaterials.* Biotechnology and bioengineering, 1994. **43**(8): p. 781-91.

10. Dunn, M.G., et al., *Anterior cruciate ligament reconstruction using a composite collagenous prosthesis. A biomechanical and histologic study in rabbits.* The American Journal of Sports Medicine, 1992. **20**(5): p. 507-15.

11. Altman, G.H., et al., *Silk matrix for tissue engineered anterior cruciate ligaments.* Biomaterials, 2002. **23**(20): p. 4131-41.

12. Li, W.J., et al., *Engineering controllable anisotropy in electrospun biodegradable nanofibrous scaffolds for musculoskeletal tissue engineering.* Journal of Biomechanics, 2007. **40**(8): p. 1686-93.

13. Freeman, J.W., et al., *Evaluation of a hydrogel-fiber composite for ACL tissue engineering.* Journal of Biomechanics, 2011. **44**(4): p. 694-9.

14. Cooper, J.A., Jr., et al., *Biomimetic tissue-engineered anterior cruciate ligament replacement.* Proceedings of the National Academy of Sciences of the United States of America, 2007. **104**(9): p. 3049-54.

15. Tischer, T., et al., *Tissue engineering of the anterior cruciate ligament: a new method using acellularized tendon allografts and autologous fibroblasts.* Archives of orthopaedic and trauma surgery, 2007. **127**(9): p. 735-41.

16. Cartmell, J.S. and M.G. Dunn, *Development of cell-seeded patellar tendon allografts for anterior cruciate ligament reconstruction.* Tissue engineering, 2004. **10**(7-8): p. 1065-75.

17. Tischer, T., et al., *Tissue engineering of the anterior cruciate ligament-sodium dodecyl sulfate-acellularized and revitalized tendons are inferior to native tendons.* Tissue engineering. Part A, 2010. **16**(3): p. 1031-40.

18. Spalazzi, J.P., et al., *Development of controlled matrix heterogeneity on a triphasic scaffold for orthopedic interface tissue engineering.* Tissue engineering, 2006. **12**(12): p. 3497-508.

19. Spalazzi, J.P., et al., *In vivo evaluation of a multiphased scaffold designed for orthopaedic interface tissue engineering and soft tissue-to-bone integration.* Journal of biomedical materials research. Part A, 2008. **86**(1): p. 1-12.

20. Mascarenhas, R., *Anterior cruciate ligament reconstruction: a look at prosthetics-past, present and possible future.* McGill Journal of Medicine, 2008. **11**(1): p. 29-37.
21. Frank, C.B. and D.W. Jackson, *The science of reconstruction of the anterior cruciate ligament.* The Journal of bone and joint surgery. American volume, 1997. **79**(10): p. 1556-76.
22. Wang, I.E., et al., *Role of osteoblast-fibroblast interactions in the formation of the ligament-to-bone interface.* Journal of orthopaedic research : official publication of the Orthopaedic Research Society, 2007. **25**(12): p. 1609-1620.
23. Cooper, J.A., Jr., et al., *Evaluation of the anterior cruciate ligament, medial collateral ligament, achilles tendon and patellar tendon as cell sources for tissue-engineered ligament.* Biomaterials, 2006. **27**(13): p. 2747-54.
24. Fan, H., et al., *Anterior cruciate ligament regeneration using mesenchymal stem cells and silk scaffold in large animal model.* Biomaterials, 2009. **30**(28): p. 4967-77.
25. Alhadlaq, A. and J.J. Mao, *Mesenchymal stem cells: isolation and therapeutics.* Stem cells and development, 2004. **13**(4): p. 436-448.

26. Stoltz, J.F., et al., *Cell and tissue engineering and clinical applications: an overview.* Bio-medical materials and engineering, 2006. **16**(4 Suppl): p. S3-S18.

27. Van Eijk, F., et al., *Tissue engineering of ligaments: a comparison of bone marrow stromal cells, anterior cruciate ligament, and skin fibroblasts as cell source.* Tissue engineering, 2004. **10**(5-6): p. 893-903.

28. Caplan, A.I., *Adult mesenchymal stem cells for tissue engineering versus regenerative medicine.* Journal of cellular physiology, 2007. **213**(2): p. 341-347.

29. Pittenger, M.F., et al., *Multilineage potential of adult human mesenchymal stem cells.* Science (New York, N.Y.), 1999. **284**(5411): p. 143-147.
30. Dezawa, M., et al., *Bone marrow stromal cells generate muscle cells and repair muscle degeneration.* Science (New York, N.Y.), 2005. **309**(5732): p. 314-317.

31. Moreau, J.E., et al., *Growth factor induced fibroblast differentiation from human bone marrow stromal cells in vitro.* Journal of orthopaedic research